EFFECTS OF SOLAR VARIABILITY ON COSMIC RAY INTENSITY

DISSERTATION

SUBMITTED IN PARTIAL FULFILMENT OF THE REQUIREMENTS
FOR THE AWARD OF THE DEGREE OF

Master of Philosophy

IN

PHYSICS

BY

VIVEK GUPTA

Under the Supervision of

DR. BADRUDDIN

DEPARTMENT OF PHYSICS
ALIGARH MUSLIM UNIVERSITY
ALIGARH (INDIA)

2005

Dr. Badruddin
Reader

Department of Physics
Aligarh Muslim University, Aligarh-202002

Phone: 0571-2701001(O)
: 0571-2720162(R)
Fax : 0571-2700093
: 0571-2701001
e-mail:

Dated:

CERTIFICATE

I certify that the **M. Phil. dissertation** entitled ***"Effects of Solar Variability on Cosmic Ray Intensity"*** is based on the original research work carried out by **Mr. Vivek Gupta** under my guidance.

(Dr. Badruddin)
Supervisor

Acknowledgement

I express my sincere gratitude to my supervisor, **Dr. Badruddin**, for providing his guidance, kind support and blessings: all the ingredients necessary for this work.

I am thankful to **Prof. Muhammad Irfan**, Chairman, Department of Physics for providing necessary facilities in the Department.

I am also thankful to **Dr. Abbas Ali** and **Prof. Wasi Haider** for their kind support.

I also wish to thank **my colleagues** who helped me directly or indirectly in the accomplishment of this work.

-Vivek Gupta

(nucleus12@rediffmail.com)

CONTENTS

Chapter-I

The Solar Wind, the Heliosphere and the Cosmic Rays

1.1 The Solar Wind

1.2 Parker' Model of the Solar Wind

1.3 Basic Nature of the Interplanetary Magnetic Field

1.4 High Speed Solar Wind Streams

1.4.1 The Connection between Corona Structure and Solar Wind Stream Structure

1.4.2 Solar Cycle Effects

1.5 Corotating Interaction Regions (CIRs)

1.6 The Heliosphere

1.7 The Heliospheric Current Sheet

1.7.1 Relation to the Solar magnetic Field and the Streamer Belt

1.7.2 Energetic Particles in the Heliosphere

1.7.3 Importance and Implications

1.8 Cosmic Ray Modulation

1.8.1 Transport Equation

1.8.2 Modulation Physics: Current View

Chapter-II

Solar Plasma/Field and Cosmic Ray Variations

2.1 Introduction

2.2 Method of Analysis

2.3 Results and Discussion

2.4 Conclusions

References

Chapter - I

The Solar Wind, the Heliosphere and the Cosmic Rays

CHAPTER-I

THE SOLAR WIND, THE HELIOSPHERE AND THE COSMIC RAYS

1.1 The Solar Wind

The Earth's atmosphere is stationary, shaped by equilibrium between incoming solar radiation and outgoing terrestrial radiation. On the Sun, the situation is different. Here the temperature is much higher and the solar atmosphere is not stable but blown away as solar wind, filling the entire heliosphere.

The solar wind is plasma, i. e., an ionized gas that permeates interplanetary space. It exists as a consequence of the supersonic expansion of the sun's hot outer atmosphere, the corona. The solar wind consists primarily of electrons and protons, but alpha particles and many other ionic species are also present at low abundance levels. At the orbit of earth, 1 AU from the sun, typical solar wind densities, flow speeds, and temperatures are of the order of 8 protons cm^{-3}, 470 km s^{-1} and 1.2 x 10^5 K respectively; hoever, the solar wind is highly variable in both space and time. A weak magnetic field embedded within the solar wind plasma is effective both in excluding some low-energy cosmic rays from the solar system and in channeling energetic particles from the sun in to interplanetary space. The solar wind plays an essential role in shaping and stimulating planetary magnetospheres and the ionic tails of comets.

1.2 Parker's Model of the Solar Wind

Eugene Parker, in 1958, formulated a theoretical model of the solar corona that proposed that the solar atmosphere is continually expanding into interplanetary space. Prior to Parker's work most theories of the solar atmosphere treated the corona as static and gravitationally bound to the Sun.

His consideration of the hydrodynamic (i.e., fluid) equations for mass, momentum, and energy conservation for a hot solar corona led him to unique solutions for the coronal expansion that depended on the value of the coronal temperature close to the surface of the Sun. The expansion produced low flow speeds close to the Sun, supersonic flow speeds (i.e., flow speeds greater than the speed with which sound waves propagate) far from the Sun (Figure 1.1), and vanishingly small pressures at

large heliocentric distances. In view of the fluid character of the solutions, Parker called this continuous, supersonic, coronal expansion the "solar wind".

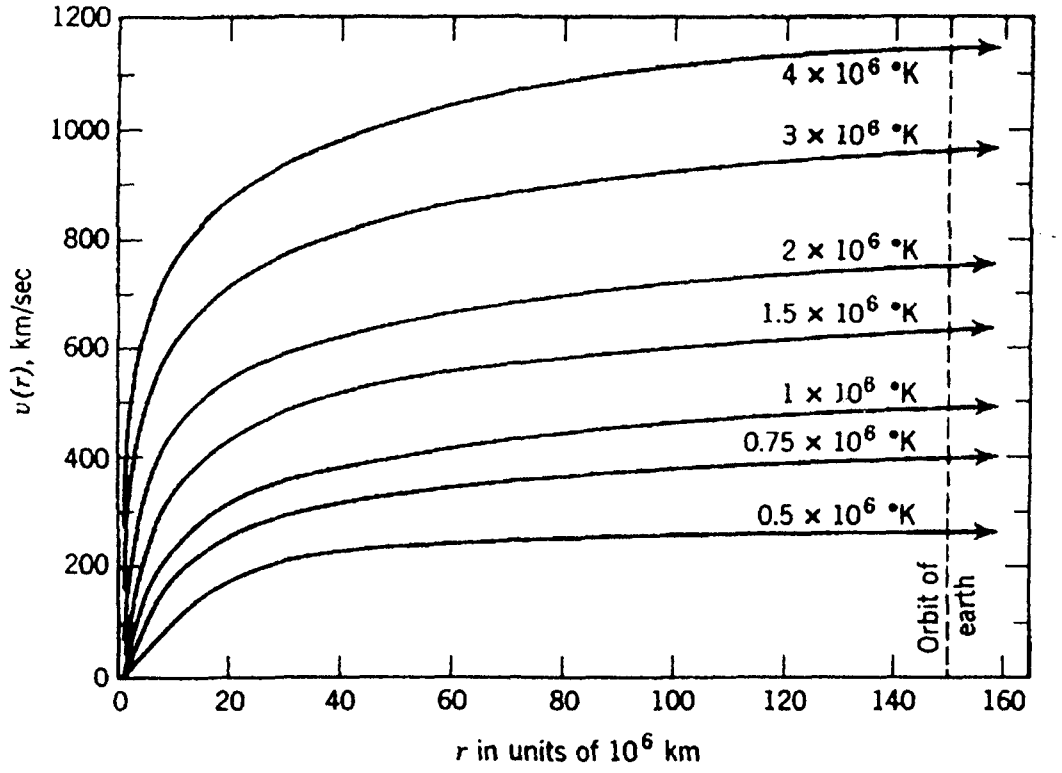

Fig. 1.1: Solar wind speed variation from the sun as obtained by Parker

1.3 Basic Nature of the Interplanetary Magnetic Field

In addition to being a very good thermal conductor, the solar wind plasma is an excellent electrical conductor. Indeed, the electrical conductivity of the plasma is so high that the solar magnetic field is "frozen" into the solar wind flow as it expands away from the Sun. Because the Sun rotates, field lines in the equatorial plane of the Sun are bent into spirals (Fig. 1.2) whose inclinations relative to the radial direction depend on heliocentric distance and the speed of the solar wind. Each field line threads plasma, emitted from a single point on the Sun. At 1 AU the average field line spiral in the equatorial plane is inclined -45 deg to the radial direction from the Sun.

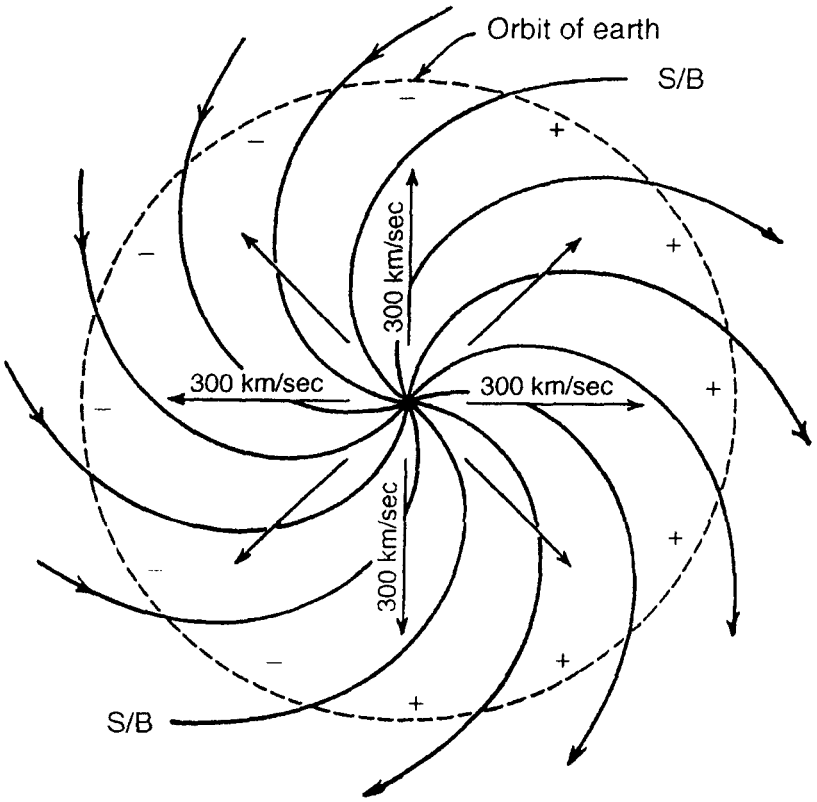

Fig. 1.2: Parker's spiral magnetic field

In Parker's simple model interplanetary magnetic field lines out of the equatorial plane take the form of helixes wrapped about the rotation axis of the Sun. These helixes are ever more elongated at higher solar latitudes and eventually approach radial lines over the poles of the Sun. The equations describing Parker's model of the interplanetary magnetic field far from the Sun are

$$B_r(r,\phi,\theta) = B(r_o,\phi_o,\theta)\,(r_o/r)^2,$$

$$B_\phi(r,\phi,\theta) = -B(r_o,\phi_o,\theta)\,(\omega r_o^2/V_{sw}r)\sin\theta,$$

$$B_\theta = 0.$$

Here r, ϕ, θ are.radial distance, longitude, and latitude in a Sun-centered spherical coordinate system, B_r, B_ϕ and B_θ are the magnetic field components in this coordinate system, ω is the angular velocity associated with solar rotation (2.9×10^{-6}

radians sec $^{-1}$), V_{sw} is the solar wind fow speed (assumed constant with distance from the Sun), and ϕ_0 is an initial longitude at a reference distance r_o from Sun center.

Parker's model is in reasonably good agreement with suitable averages of the magnetic field measured in the ecliptic plane and at high latitudes over a wide range of heliocentric distances. However, the instantaneous orientation of the field often deviates substantially from the model field at all latitudes. Moreover, there is evidence that interplanetary magnetic field lines commonly wander in latitude as they extend out into the heliosphere. This effect appears to be a result of motion of the foot points of the field lines on the surface of the Sun associated with both differential solar rotation (the surface of the Sun rotates at different rates at different latitudes) and turbulent convective motions (Kallenrode, 1998).

1.4 High Speed Solar Wind Streams

Solar wind is far from homogeneous due to the great amount of coronal structure. In fact, observations reveal that the solar wind in the ecliptic plane tends to be organized into alternating streams of high and low speed flows.

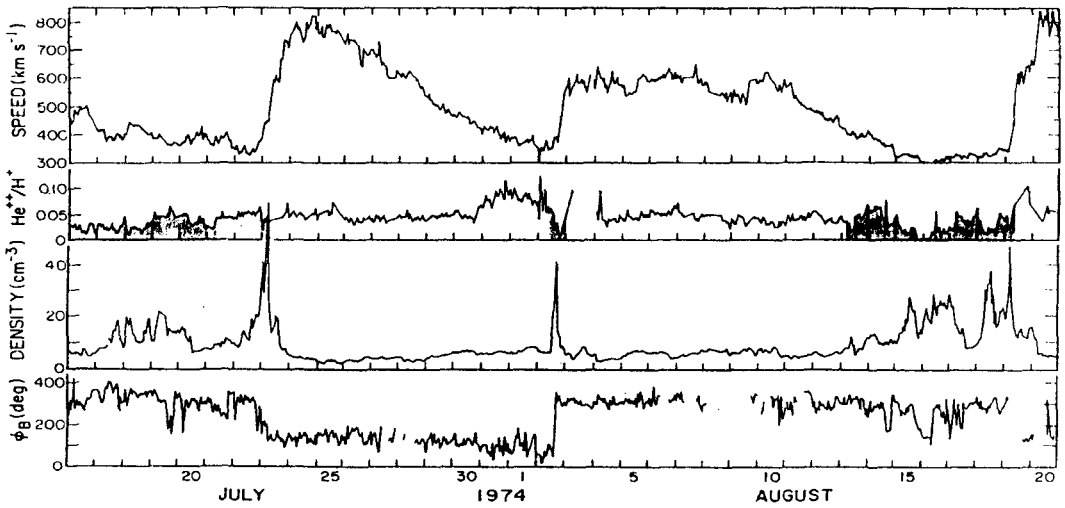

Fig. 1.3: Solar wind properties during high-speed streams

Fig. 1.3, which shows time histories of selected solar wind parameters at 1 AU for a 36-day interval in 1974, illustrates certain characteristic aspects of this stream structure that are particularly prevalent during the declining phase of the ~ll-yr solar activity cycle. From top to bottom the figure shows solar wind flow speed, the helium

abundance relative to hydrogen, the proton density, and the azimuthal angle, ϕ_B, of the interplanetary magnetic field (relative to an inward directed radial) plotted versus time. Three high-speed streams, which began on July 22, August 2, and August 19 and which persisted for a number of days each, are clearly evident in the figure. The July 22 and August 19 streams are actually the same stream encountered on successive solar rotations. For each stream the maximum speed exceeds 600 km s^{-1}, while between streams the speed falls to values below 350 km s^{-1}. Each high-speed stream is unipolar in the sense that ϕ_B is roughly constant throughout the stream. During the streams that began on July 22 and August 19 ϕ_B is approximately 135 deg, indicating that the field is directed outward away from the Sun along the interplanetary spiral. In contrast, during the intervening stream ϕ_B is approximately 315 deg, and the field is directed inward toward the Sun along the spiral. Sharp, long-lived reversals in field polarity occur at low speeds close to the leading edges of the high-speed streams, while more transient reversals occur elsewhere within the low speed flows. The polarity reversals at the leading edges of the streams correspond to crossings of the heliospheric current sheet (Gosling, 1996).

Variations in solar wind density are closely coupled to the field and flow structure. Particularly large and well-defined peaks in density occur in coincidence with the heliospheric current sheet crossings on July 23, August 2, and August 19. Smaller peaks in density occur in the low-speed solar wind that are loosely associated with more transient reversals in field polarity. The density tends to be lowest within the cores of the high-speed streams. Within the high-speed streams the helium abundance, A(He), is roughly constant at a value of about 4.5%, while within the low speed flows A(He) is more variable, but tends toward lower values than within the cores of the high-speed streams. Relative minimums in A(He) occur at crossings of the heliospheric current sheet.

1.4.1 The Connection between Corona Structure and Solar Wind Stream Structure

Fig. 1.4 provides a schematic illustration of the connection between solar wind stream structure and coronal structure. Quasi-stationary high-speed streams originate in coronal holes (see Fig 1.5 which shows various features of the sun including polar coronal hole), which are large, nearly unipolar regions in the solar atmosphere.

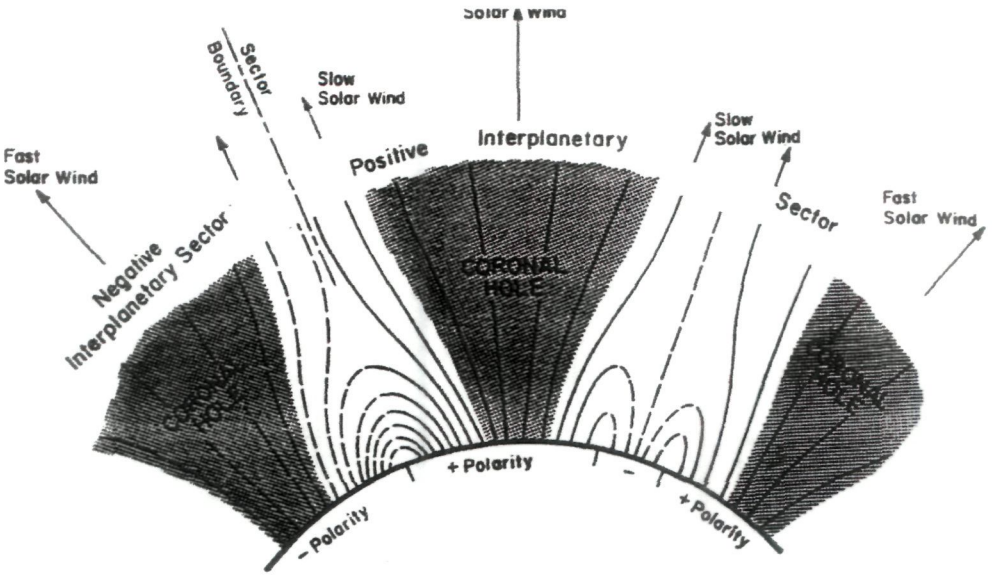

Fig. 1.4: Connection between solar stream structure and coronal structure

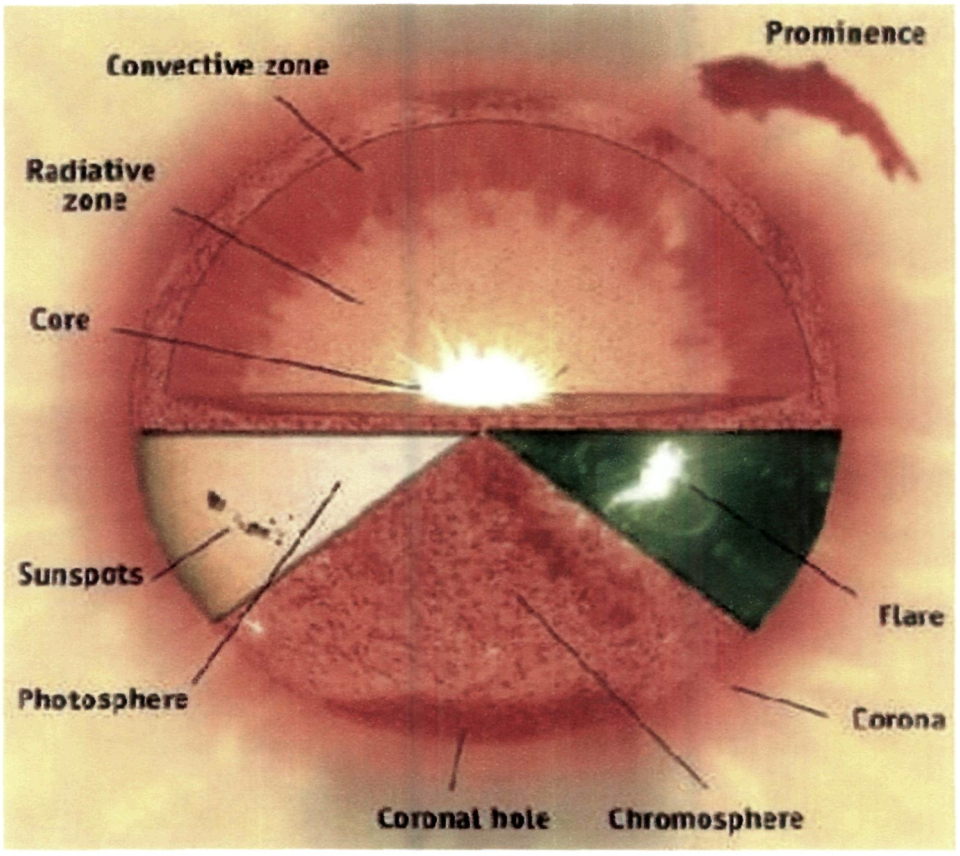

Fig. 1.5: The Sun and its atmosphere

The coronal density is relatively low within coronal holes because the solar wind expansion there is relatively unconstrained by the solar magnetic field. Low-speed flows, on the other hand, originate in the outer portions of coronal streamers that straddle regions of magnetic field polarity reversals. Close to the surface of the Sun within coronal streamers the magnetic field is strong, field lines are entirely closed, the solar wind expansion is choked off, and coronal densities are high. At higher altitudes within streamers the field is weaker and can be opened up by the coronal plasma pressure, producing the relatively dense, slow-speed flows at 1 AU characteristic of the region surrounding polarity reversals in the magnetic field.

1.4.2 Solar Cycle Effects

The corona continually evolves in response to the changing solar magnetic field associated with the advance of the ~11-year solar activity cycle. Near solar activity minimum and on the declining phase of the solar cycle large coronal holes are found near the solar magnetic poles that often extend down to low heliographic latitudes. Thus quasi-stationary high-speed streams are common in the ecliptic plane at these times. Near solar activity maximum, however, strong magnetic fields choke off the coronal expansion over much of the Sun, and the solar wind flow in the ecliptic tends to be slower and more variable, often being disrupted by transient events associated with solar activity.

1.5 Corotating Interaction Regions (CIRs)

The solar wind at low heliographic latitudes tends to be structured into alternating streams of high and low speed flows that corotate with the Sun, particularly on the declining phase of the ~11-year solar activity cycle. This structure is a consequence of the fact that the solar wind expansion is modulated by the Sun's magnetic field. The high-speed streams originate in coronal holes that extend equatorward from the magnetic poles of the sun, while the low-speed streams originate in the outer portions of the dense coronal streamers that tend to straddle the solar magnetic equator. At low solar latitudes solar rotation causes high-speed plasma to be directed in the same radial direction and behind slow solar wind plasma originating from regions to the west (as viewed from Earth the Sun rotates from east to west, i.e., in the same sense as planetary motion about the Sun, at a rate of ~13.3/day). With

increasing distance from the Sun the high-speed streams steepen and overtake the slower plasma ahead, producing compressive CIRs on the leading edges of these streams. A CIR is a region of high pressure; its leading edge is a forward wave that propagates into the slow solar wind ahead of a high-speed stream, while the trailing edge is a reverse wave that propagates back into the stream itself (Fig. 1.6). These waves commonly steepen into forward and reverse shocks that bound the CIR at heliocentric distances beyond ~2 AU. Slow solar wind plasma is accelerated as it encounters the forward wave, while fast solar wind plasma is decelerated as it encounters the reverse wave. The effect of a CIR is thus to limit the steepening of a high-speed stream and to transfer momentum and energy from the stream to the slower-moving plasma ahead. This is the prime mechanism by which solar wind speed differences are reduced with increasing distance from the Sun (Barnes, 1992).

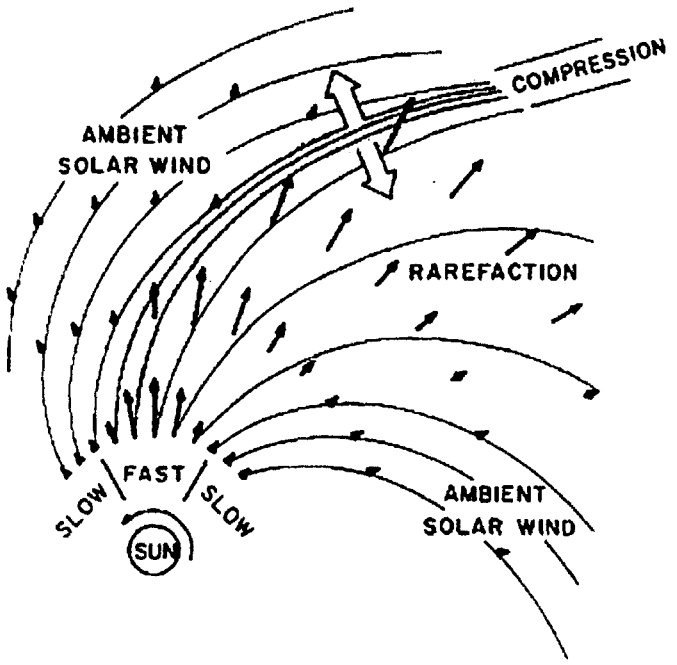

Figure 1.6: Formation of a corotating interaction region

Our understanding of CIRs has essentially been two-dimensional; i.e., we understood the basic structure and evolution of CIRs as functions of radius and longitude, but lacked information on their structure and evolution as a function of solar

latitude. For example, the process of stream steepening with increasing distance from the Sun and the subsequent formation of forward-reverse shock pairs was well understood, and it was generally appreciated that solar rotation causes CIRs in the solar equatorial plane to take the form of Archimedean spirals (defined by $\mathbf{r} = \mathbf{v}\,\varphi / \Omega$ where **r** is heliocentric distance, **v** is the solar wind speed, $\varphi$is solar longitude, and Ω is the angular rotation rate of the Sun) whose pitches relative to the radial direction are intermediate between those associated with the high-speed streams and those associated with the low-speed plasma ahead of the streams.

1.6 The Heliosphere

The heliosphere is the region of space in which the pressure of the solar wind exceeds the pressure of the streaming interstellar wind. The supersonic solar wind, consisting mainly of protons, electrons, and alpha particles, radially expands in all directions, carrying with it the solar magnetic field.

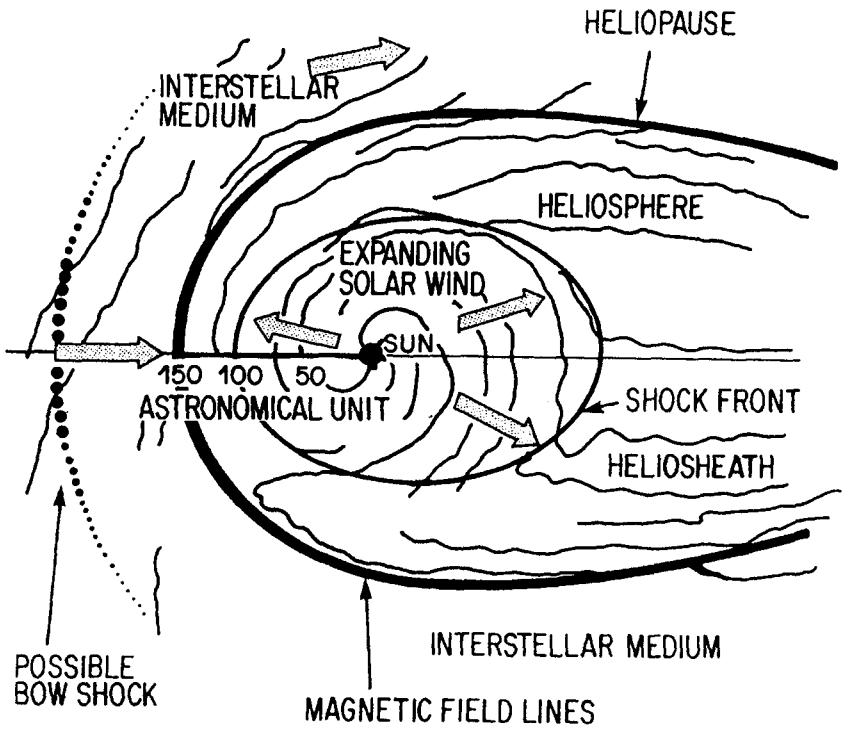

Fig. 1.7: A schematic view of the heliosphere and its interaction with the local interstellar medium.

This wind creates a gigantic bubble (the heliosphere) in the interstellar medium (Fig. 1.7). The size of the heliosphere is not presently known with certainty, but it extends well beyond the orbit of Pluto (Venkatesan and Badruddin, 1990). The heliosphere is a region dominated by solar activity. Thus the importance of the solar control and influence on diverse phenomena within this region has come to be recognized.

The motion of the solar system in the interstellar medium could generate a bow shock. Figure 1.8, which gives a conceptual overview of the heliosheath, and heliopause, is reminiscent of the terrestrial magnetosphere. The region between the bow shock and the boundary of the heliosphere (heliopause) contains the interstellar magnetic field (I 0^{-6} G). The continuous outpouring of solar wind at supersonic speed is anticipated to become subsonic outside the heliopause. Within the region of the shock front, the magnetic field traces the so-called archimedian spiral. The plasma flow is radial. Outside the shock front, the magnetic fields are visualized as disordered and the plasma flow as turbulent.

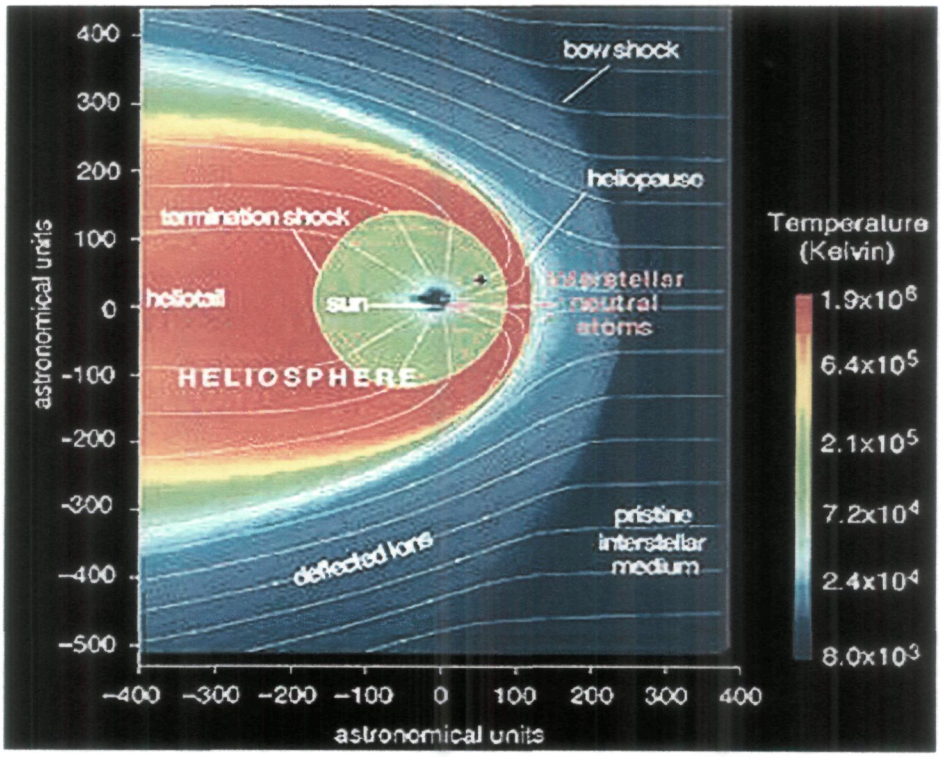

Fig. 1.8: A view of the heliosphere showing distances of various structures

Earth and all the other planets orbit within the heliosphere, and many satellites have been launched around the Earth. It was at first thought that the heliosphere was spherical in shape. However, by study of the motion of stars nearby, it has been found that the local interstellar medium flows past the Sun (from the general direction of the galactic center) with a speed of about 26 km/s.

The first suggestions concerning the existence and nature of the heliosphere were made in 1955 by Leverett Davis in connection with the origin and propagation of cosmic rays. The essential element was that "solar corpuscular radiation" (termed the "solar wind" in 1958 by Eugene Parker) would force matter and magnetic flux in the local interstellar medium outward, thereby partially excluding cosmic rays. The simplest expression of the concept is that the solar wind blows a spherical bubble, the "heliosphere," that continually expands over the lifetime of the solar system. However, if there is a significant pressure in the interstellar medium, the expansion must eventually stop.

Kurth and Gurnett (1991) have estimated the distance of the heliospouse using the data of radio emissions thought to emanate from the heliopause; these were registered by detectors on both Voyager 1 and 2. They estimated that the distance of the heliopause is between 116 and 177 AU from the Sun.

The heliosphere is actually a semi-permeable body. The magnetized interstellar plasma is unable to enter this body but dust, neutral atoms and galactic cosmic rays (GCR) can cross the heliopause and penetrate deeply into the heliosphere. Hydrogen atoms penetrate to within only ~5 AU of the Sun before becoming ionized by short wavelength solar radiation or by giving up an electron to a solar wind ion (charge exchange). The atoms have so little mass that the inward force due to solar gravity is nearly compensated by the outward solar radiation pressure, which increases the probability of ionization before the atoms reach the inner heliosphere. Neutral helium, on the other hand, being more massive and harder to ionize, can penetrate nearer the Sun and has been detected at 1 AU.

1.7 The Heliospheric Current Sheet

Along the plane of the Sun's magnetic equator, the oppositely directed open field lines run parallel to each other and are separated by a thin current sheet known as the "interplanetary current sheet" or "heliospheric current sheet". The current sheet is

tilted (because of an offset between the Sun's rotational and magnetic axes) and warped (because of a quadrupole moment in the solar magnetic field) and thus has a wavy, "ballerina skirt"-like structure as it extends into interplanetary space. Because the Earth is located sometimes above and sometimes below the rotating current sheet, it experiences regular, periodic changes in the polarity of the IMF. These periods of alternating positive (away from the Sun) and negative (toward the Sun) polarity are known as magnetic sectors (Smith, 1993).

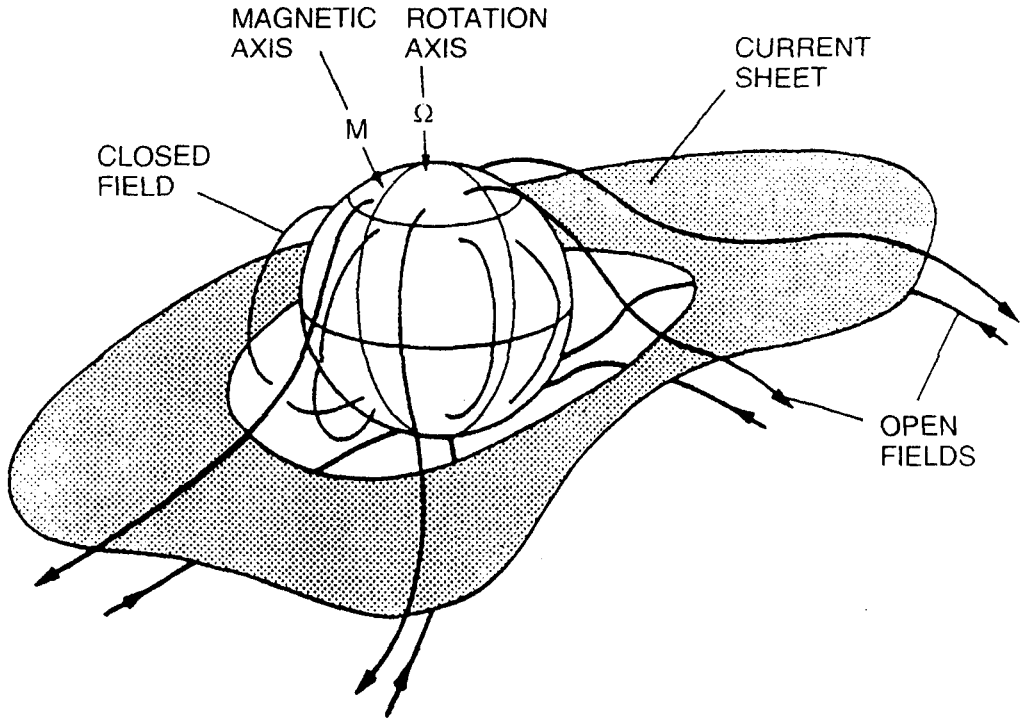

Fig. 1.9: Schematic of the heliospheric current sheet. The shaded current sheet separates fields from the north and south solar magnetic poles.

The Heliospheric Current Sheet, or HCS, is the boundary encircling the Sun that separates oppositely directed magnetic fields that originate on the Sun and are "open" (only one end is attached to the Sun) (Fig. 1.9). These fields are closely associated with the Sun's dipole magnetic field and have opposite magnetic polarities, e.g., outward (positive) in the north and inward (negative) in the south. The current sheet separates these oppositely directed fields as required by Maxwell's equations, with the vector difference between the fields on the two sides being a measure of the

linear current density. If it were not for the underlying simplicity of the heliospheric magnetic field being dipole-like, there might have been several current sheets surrounding the Sun, and HCS would be less distinctive. As it is, the HCS is unique and represents the magnetic equator of the global heliosphere.

1.7.1 Relation to the Solar Magnetic Field and the Streamer Belt

Polarity reversals in the interplanetary magnetic field correspond to crossings of the heliospheric current sheet map to the centers of coronal streamers. Coronal streamers, in turn, lie above regions in the lower solar atmosphere where the solar magnetic field reverses direction. On the declining phase of the solar activity cycle and near solar activity minimum the Sun's large-scale magnetic field is approximately that of a dipole, similar to the Earth's. Regions where the Sun's field reverses direction from outward to inward and vice versa correspond approximately to the solar magnetic equator. Just as the Earth's magnetic dipole is tilted relative to the Earth's rotation axis, so too is the solar magnetic dipole tilted with respect to the Sun's rotation axis. (The Sun's rotation axis, in turn, is tilted approximately 7 deg relative to ecliptic north.)

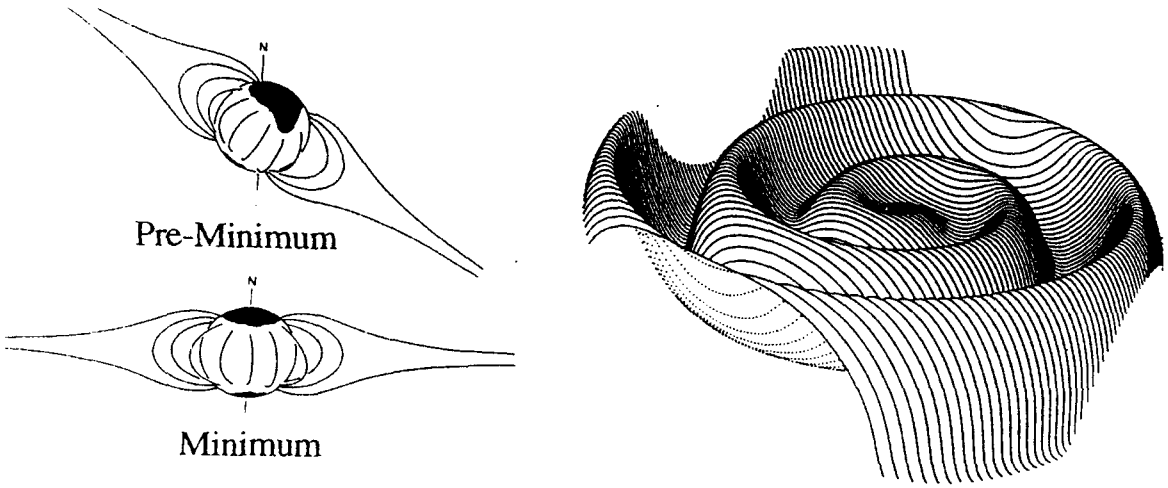

Fig. 1.10: Alignment of magnetic dipole relative to rotation axis (left) and tilt in HCS (right)

However, the orientation of the solar magnetic dipole relative to the solar rotation axis is considerably more variable in time than is the orientation of the Earth's magnetic dipole relative to its rotation axis. As illustrated in the lower left portion of Fig. 1.10,

near solar activity minimum the solar magnetic dipole tends to be aligned nearly with the rotation axis, while on the declining phase of the activity cycle it is generally inclined at a considerably larger angle relative to the rotation axis. Near solar maximum the Sun's field is not well approximated by a dipole.

1.7.2 Energetic Particles in the heliosphere

A proton moving with the average solar wind speed of 400 km s^{-1} has energy of 0.84 k eV, while an alpha particle moving with same speed has energy of 3.4 k eV. Thus, by most measures solar wind ions are low energy particles. Interplanetary space is, nevertheless, filled with a number of energetic particle populations. Except in restricted regions of space, such as immediately in front of the planetary bow shocks or in the outer heliosphere close to the termination shock, the energetic particles found in the solar wind have insufficient energy densities to alter the bulk motion of the plasma or affect the overall strucmre of the interplanetary magnetic field. Thus, for the most part, energetic particles in the solar wind behave as test particles whose motions are guided and controlled by the interplanetary magnetic field.

1.7.3 Importance and Implications

As long as the sectors were axially aligned with the Sun's rotation axis, their effect on cosmic rays was expected to "average out," and they were thought to be of little or no significance. However, an inclined current sheet would have a significant effect on the global heliospheric field and on the drift motions of the cosmic rays. These implications were pointed out by R. Jokipii and his colleagues, who proceeded to include drift effects in the basic transport equation used to describe the behavior of energetic particles (Jokipii et al., 1977). In particular, the HCS was shown to cause fast drifts along it and to act as a major "source" or "sink" of cosmic rays in the heliosphere (depending on the polarity of the fields above and below it, which change sign from one sunspot cycle to the next). The influence of the HCS was evident in the model as a correlation between cosmic ray intensity and the changing inclination of the current sheet. This aspect of the model was shown to be consistent with observations (Smith, 1990).

Knowledge as to whether solar wind streams originate above or below the HCS, i.e., their polarity, is useful in many circumstances. An example is the

investigation of corotating interaction regions (CIRs), in which a sequence of streams are to be sorted out or merged interaction regions are to be identified along with their constituent streams. Studies of solar wind structures at widely separated locations in the heliosphere also frequently benefit from knowing the magnetic polarities of the structures.

The HCS also represents an example of a basic plasma structure in the heliosphere. From this point of view it is an important example among many other current sheets observed in space such as solar wind discontinuities or current sheets embedded in cometary or magnetospheric tails. Localized current sheets also occur on the Sun and are considered an essential feature of isolated coronal streamers.

1.8. Cosmic Ray Modulation

Forbush (1954) was the first to report that the intensity of the cosmic radiation measured at Earth varies systematically in anti-correlation with the solar activity during the 11-year solar activity cycle. As shown in Fig. 1.11, which contains the record of the smoothed sunspot number and the variation in the cosmic ray intensity.

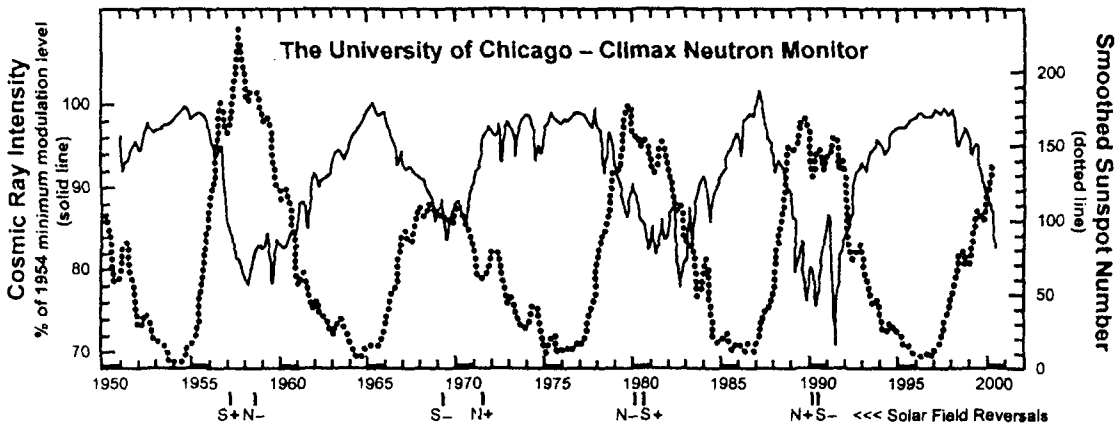

Fig. 1.11: Solar activity and cosmic ray intensity variations

Intensity variations are caused by variations in the effectiveness of the solar wind in excluding cosmic rays from the inner solar system as a result of changes in the structure of the solar wind and interplanetary magnetic field with the level of solar

activity, and there is by now a basic understanding of, and some rather detailed models for, the physical processes that produce modulation of the cosmic ray intensity by the solar wind. However, as we still have only partial knowledge of the structure of the heliosphere and of its variations during the solar cycle, our picture of modulation is not yet complete (Mckibben et al., 1995).

1.8.1 Transport Equation

Within the heliosphere, cosmic-ray particles are being transported in a magnetic field which is a function of position and time, and which is frozen into the outward-moving plasma. These particles are subjected to four distinct transport effects, which contribute to two distinct kinds of motion. There is a general guiding center motion, which occurs at the same time as a random walk or spatial diffusion. More specifically, since the particles tend to stay on a given field line, they are convected with the fluid flow. The magnetic field varies systematically over large scales, so there are, in addition, curvature and gradient drifts, which are coherent over large distances. Because of the V x B electric field of the wind, there are associated energy changes. The scattering causes the random walk or spatial diffusion by random magnetic irregularities (Jokipii, 1989; Potgieter, 1998).

The resulting transport is a superposition of these coherent and random effects. They were combined first by Parker (1965), to obtain the generally accepted transport equation for the quasi-isotropic distribution function f(r, p, *t)* of cosmic rays of momentum *p* at position r and time *t.*

$$\frac{\partial f}{\partial t} = \frac{\partial}{\partial x_i}\left[k_{ij}\frac{\partial f}{\partial x_i}\right] \qquad (diffusion)$$

$$-U_i \frac{\partial f}{\partial x_i} \qquad (convection)$$

$$-V_{di}\frac{\partial f}{\partial x_i} \qquad (guiding-center\ drift)$$

$$+\frac{1}{3}\frac{\partial U_i}{\partial x_i}\left[\frac{\partial f}{\partial \ln p}\right] \qquad (energy\ change)$$

$$+Q(x_i, t, p) \qquad (source)$$

The labels next to each of the various terms indicate the associated physical effect. The guiding center drift velocity is given in terms of the local magnetic field B and the particle charge q by $V_d = (pcw/3q) \nabla \times (B/B^2)$. This transport equation has been used in most discussions of cosmic-ray transport and acceleration over the past two decades. It appears that it is a good approximation if there is enough scattering by the magnetic irregularities to keep the distribution function nearly isotropic. Moreover, it requires that the particles have random speeds substantially larger than the background fluid convection speed. In particular, the velocity need not be a continuous function of position. Shocks can be discussed within the framework of this equation and all that happens is that the divergence of the velocity of the flow velocity in this part of the equation becomes a delta function. In fact all of the standard theory of diffusive shock acceleration is contained in this equation.

Earl et al. (1988) added terms involving viscosity and inertial effects to obtain a more general transport equation. However, these new effects, which in general must be included, may be shown to be small in the modulation problem.

Charged particles such as cosmic rays are deflected by magnetic fields. There is the galactic magnetic field, interstellar magnetic fields, the solar magnetic field and of course Earth's magnetic field. Therefore it is impossible to determine the origin of galactic cosmic rays via the incoming direction. GCR's are first deflected by the galactic magnetic field and interstellar magnetic fields, when they enter our solar system they are deflected by the solar magnetic field and if they come near Earth they are even more deflected by Earth's magnetic field. These magnetic fields are not constant, but vary with time, especially the latter two. Furthermore there are local variations of the magnetic field in the solar system (long term: solar cycle; short term: magnetic clouds produced by solar flares) and of Earth's magnetic field caused by variations of the solar wind.

Galactic cosmic rays, deflected by solar/interplanetary magnetic field, are observed to vary over short-term (hours to day) and long-term (11-year and 22-year).

1.8.2 Modulation Physics: Current View

The heliosphere is the region of space dominated by the solar wind. First suggested to explain ground-based observations of solar energetic particles from the February 1956 solar flare (Meyer et al., 1956) the heliosphere was originally pictured

as a spherical shell of tangled magnetic fields surrounding the sun at a radius of a few AU. Since then our understanding of the heliosphere and its structure has developed greatly as spacecraft have pushed our observational knowledge to larger radii (with V1, V2, P10 and P11) and higher latitudes (with *Ulysses)* and as observations have accumulated over a number solar cycles with increasingly sophisticated instrumentation.

The basic physics of solar modulation is well known and has been the subject of several several reviews *(e. g.* Kota, 1989; McKibben, 1988 and 1990; Venkatesan and Badruddin, 1990; Potgieter 1998).

Early models of the modulation considered only diffusion, convection, and adiabatic deceleration, assumed quasi-steady conditions in a spherically symmetric heliosphere, and postulated only simple variations of the parameters (e.g. diffusion coefficients) within the heliosphere. Since the intensity at any one point depends only on the integral of the modulation effects along the path of the particles, these models gave useful first-order results for understanding the modulation as observed at Earth. As spacecraft began to travel ever further from Earth in the heliosphere, however, such models became inadequate to describe the increasingly detailed observations of the temporal and spatial dependence of the cosmic ray intensity. Among the first discoveries when spacecraft left the vicinity of Earth were that the modulation region in the heliosphere is very big, and that changes in modulation propagate outwards at the solar wind velocity.

While drifts had been neglected in early models, recognition of the existence of the large scale magnetic structure of the heliosphere, consisting of hemispheres of opposite magnetic polarity separated by a wavy current sheet that is near-equatorial at solar minimum, but that is deeply convoluted and extends to high latitudes at solar maximum, led to the suggestion that the gradient and curvature drifts in the interplanetary magnetic field could play an important role in guiding the propagation of cosmic rays through the heliosphere (Jokipii et al., 1977), and thus in modulation. Since they depend upon the 3-dimensional magnetic structure of the heliosphere, inclusion of drifts requires abandonment of spherically symmetric models of modulation. In the drift models, special importance is assigned to the high latitude regions where the spiral interplanetary field lines are nearly radial and to the current sheet that separates the opposing magnetic polarities. Outside of the polar and

equatorial regions transport via drifts is primarily in the latitudinal direction, so that observations from *Ulysses* can be especially important for assessing the role of drifts in modulation. While their inclusion in modulation models was controversial at first, drift models make specific predictions concerning the behavior of cosmic ray nuclei and electrons during the 22-year solar magnetic cycle.

The importance for the solar cycle modulation of large discrete propagating disturbances in the solar wind has been recognized *(e.g.* Webber and Lockwood, 1993; McDonald et al., 1993, and included refs.). Discovered in the outer heliosphere by the Voyager and Pioneer spacecraft, these disturbances – termed Merged Interaction Regions (MIRs), and, when of global scale, Global MIRs (GMIRs) - result from the dynamical merging at large radii of interaction regions formed between solar wind streams of differing velocities, by solar-flare-induced shock waves, and by coronal mass ejections. Simple models of the response of the cosmic rays to decreased diffusion coefficients in the such structures had remarkable success in reproducing the observed time-intensity behavior of the cosmic rays over the solar cycle by using the observed interplanetary magnetic field strength as input to the models (e.g. Perko, 1993; Burlaga, et al., 1993).

The current view of modulation accepted by most investigators is that all of the above processes are important, but that their relative importance varies throughout the solar cycle. In the period near solar minimum, when the magnetic structure of the heliosphere is particularly simple and approximates the ideal of two hemispheres of opposite magnetic polarity separated by an equatorial current sheet, drifts may play an important role in the transport of cosmic rays through the heliosphere. Even here, though, as pointed out by Jokipii and Kota (1989), irregularities in the polar fields may become important enough at large radii to significantly diminish the effectiveness of drifts. In the complex magnetic structure characteristic of solar maximum, it is likely that drifts play only a small role and that modulation is dominated by large scale disturbances in the solar wind.

Chapter - II

Solar Plasma/Field and Cosmic Ray Variations

CHAPTER-II

SOLAR PLASMA/FIELD AND COSMIC RAY VARIATIONS

2.1 Introduction

As the sun rotates, the IMF and the heliosphere current sheet (HCS) also corotates with the sun. During the course of solar rotation (~27-days period) the solar wind plasma and field parameters also vary in space and time. This variability has its effect as the cosmic ray intensity in the heliosphere. The 27-day periodicity in the galactic cosmic ray (GCR) intensity was first observed by Forbush (1938). However, the association between this recurrent cosmic ray intensity modulation and heliospheric current sheet is still not clearly understood. It is also not very clear whether the drifts are important for corotating modulation or not.

Intensity of GCR entering the heliosphere is modulated as they travel through the interplanetary magnetic field (IMF) embedded in the solar wind. The large scale IMF consists of a Parker spiral, the opposite magnetic heliosphere are devided by a thin heliospheric current sheet (HCS). Polarity state of the solar polar magnetic fields and the heliospheric, changes around every solar activity maximum period. In the decade seventies (1971-1979) and nineties (1991-1999), as an example, the field is directed outward in the northern and inward in the southern magnetic hemisphere. In this configuration, referred to as $A > 0$, positively charged GCR particles drift inward at the poles and then downward from the poles toward the HCS (near the equator). In opposite polarity configuration (when the field is directed inward in the northern and outward in the southern magnetic hemisphere) as, for example in sixties (1961-1969) and eighties (1981-1989), referred to as $A < 0$, GCR particles drift inward along the HCS (near the equator) and then upward toward the poles. Thus one expects that incoming GCR particles will be affected differently by drift effects during two magnetic configuration $A > 0$ and $A < 0$. As the sun rotates with a periodicity of a ~27-days, the earth crosses the HCS once, twice, thrice etc. during a rotation period. Consequently the separation between HCS and the earth (and hence the helio-magnetic latitude) change during the course of solar rotation.

GCR intensities were found to peak near HCS and decrease with heliomagnetic latitude irrespective of the nature (from outward to inward or vice-versa) of HCS

crossings (Badruddin et al. 1985; Newkirk and Fisk, 1985). Further, the amplitude of decrease was found to be larger during $A > 0$ than $A < 0$ epochs. These observations are consistent with the stronger recurrent (~ 26-day) GCR modulation observed during $A > 0$, since sector crossings (HCS crossings) typically occur near high speed stream leading edges near solar minimum periods (Richardson et al., 1999). The observations of Badruddin et al. (1985) and Newkirk and Fisk (1985) suggest that recurrent GCR modulation near ecliptic arise because of latitudinal cosmic ray density gradient that are arranged about the tilted HCS. Heliospheric current sheet separates the two oppositely directed magnetic polarity hemispheres of the heliosphere. The angle between the plane of the current sheet and a plane that is an extension of the sun's equator is referred to as the tilt angle of HCS. Stone (1987) and Cummings and Stone (1988), from analysis based on Voyager cosmic ray measurements in a solar cycle with $A < 0$, suggested that cosmic ray flux is roughly organized by heliomagnetic latitude. On the other hand, Reames and Ng (2001) observed peak intensities near north -south crossing of HCS and valley near south north crossing of HCS, inconsistent with simple particle gradient organized around the current sheet. Zhang et al. (1995) demonstrated that recurrent cosmic ray modulations are not intimately associated with the HCS and that 26-day recurrent variations in cosmic ray intensity are not organized by heliomagnetic latitude. Thus the whole area seems to be complex and needs further investigation.

To account for the observed polarity dependent recurrent modulation (i.e. larger modulation in $A > 0$ epoch) in GCR (as observed e.g., by Badruddin et al., 1985, Richardson et al., 1999; Alania et al., 2001) Kota and Jokipii (2001) extended 3-D simulations including drifts, and considered a southward displacement of HCS, rather than a symmetric tilted dipole. Inclusion of asymmetrically placed HCS in drift models provide results that are in qualitative agreement with the finding of Badruddin et al. (1985) and Richardson et al. (1999). On the other hand, Richardson et al. (1999) suggested that epoch dependence of the particle diffusion coefficient (Chen and Bieber, 1993) may increase the effect of solar wind convection on local cosmic ray intensity during $A > 0$ epoch and that the observed dependence in response of GCR to solar wind variations is sufficient to explain the difference.

Reames and Ng (2001), whose findings regarding recurrent modulations were not consistent with the predictions of then prevailing drift models of GCR modulations,

suggested that Fisk model of solar magnetic field (Fisk, 1996) offers great potential for explaining the recurrent variations in GCR. Burger and Hitge (2004) developed a divergence free Fisk-Parker hybrid heliospheric magnetic field and studied the effect of hybrid field on GCR by solving the 3-D steady state Parker transport equation. They investigated the 26-day recurrent variations for both protons and electrons. They have shown that hybrid field reduces intensities compared to Parker field when $A > 0$. When $A < 0$, the global effect of hybrid field are almost negligible. Their model predictions are consistent with the observed results (Zhang, 1997; Paizis et al., 1999) only when drift effects are included, indicating that drifts are important for co rotating modulation.

Further investigation is, therefore, required to ascertain the status of three recently proposed models, i.e. (i) the 3-D drift model with symmetrically placed HCS, (ii) 3-D drift model with divergence free Fisk-Parker hybrid field and (iii) convection diffusion model with epoch dependence of particle diffusion coefficient, vis-à-vis the experimental results including the solar polarity dependent effect in recurrent modulation. If none of the existing models are able to explain all the observed features of recurrent modulation, Fisk model of heliospheric magnetic field may be employed, although difficult to implement (Burger and Hitge, 2004), in the 3-D modulation codes as suggested by Reames and Ng (2001). Moreover, how the 26-day recurrent modulation contributes to the global modulation and if so by which mechanism, is still not solved completely (Simnett et al., 1998). Further studies of recurrent modulation can, therefore, provide new insight into global modulation phenomenon.

2.2 Method of Analysis

The heliospheric current sheet evolves during the course of a Carrington rotation. For the study of GCR variations during Carrington rotation periods, we have adopted the method of superposed epoch analysis. Epoch (zero day/hour) corresponds to the Carrington rotation start time. Analysis has been performed during low solar activity periods; to avoid large Forbush decrease due to transient solar disturbances as they occur more frequently during or near solar maximum periods. If Forbush-type decrease occurs during a Carrington period, that rotation has been omitted from the analysis. Further, during low solar conditions, the evolution of current sheet during each Carrington rotation is relatively smooth. Due to these reasons, low/minimum solar activity periods have been selected for the analysis. GCR intensity

data of two neutron monitors, on located at Oulu (Latitude = 65.02^{O} N, Longitude = 25.50^{O} E, Cut off rigidity = 0.81 GV) and other at Climax (Latitude = 37.37^{O} N, Longitude = 106.18^{O} W, Cut off rigidity = 3.03 GV) together with solar/heliospheric plasma and field data have been utilized for the analysis. GCR intensity and solar wind data have been analyzed during; (i) minimum solar activity periods, 1976-77 (A > 0), 1985-86 (A < 0) and 1995-96 (A > 0); (ii) decreasing and low activity period in which high speed solar wind streams are more frequently observed, 1983-84 (A < 0) and 1993-94 (A > 0); (iii) combined low activity periods during decreasing and minimum solar activity, separately for each epoch 1983-86 (A < 0) and 1993-96 (A > 0) in order to increase the statistics.

2.3 Results and Discussion

The origin of recurrent modulation of GCR must be in solar wind and the interplanetary magnetic field as all the basic processes of modulation (Particle diffusion, convection, drift and adiabatic deceleration) are controlled by properties of magnetic field fluctuations, large-scale interplanetary magnetic field structures and solar wind velocity. Corotating depressions in cosmic rays have been studied in relation to solar wind plasma and field conditions (e.g. Duggal and Pomerantz, 1977; Iucci et al., 1979; Venkatesan et al., 1982; Burlaga et al., 1984; Mishra et al., 1990; Badruddin, 1993, 1997; Yadav et al., 1994; Richardson et al., 1996, 1999; Alania et al., 2001; Gil et al., 2005). However, consensus eludes the conclusion as regards the solar wind parameters playing important role in these depressions; probably due to near simultaneous variations in a number of parameters (e.g., solar wind velocity, magnetic field magnitude, magnetic turbulence etc.) observed during cosmic ray depression. As a consequence of variations in these parameters, several processes could contribute in modulation (Richardson et al., 1996; Badruddin, 1997). Charges in so1ar wind speed could cause variation in convection and adiabatic cooling, diffusion coefficient many change due to variations in turbulence level, and variation in field strength may be responsible for causing variation in diffusion coefficients and particle drifts (Richardson, 2004).

In Fig. 2.1(a, b, c) we have plotted the superposed epoch analysis results of daily average GCR intensity data of Oulu and Climax neutron monitors together with simultaneous plots of solar wind velocity (V), heliospheric magnetic field (B), it's

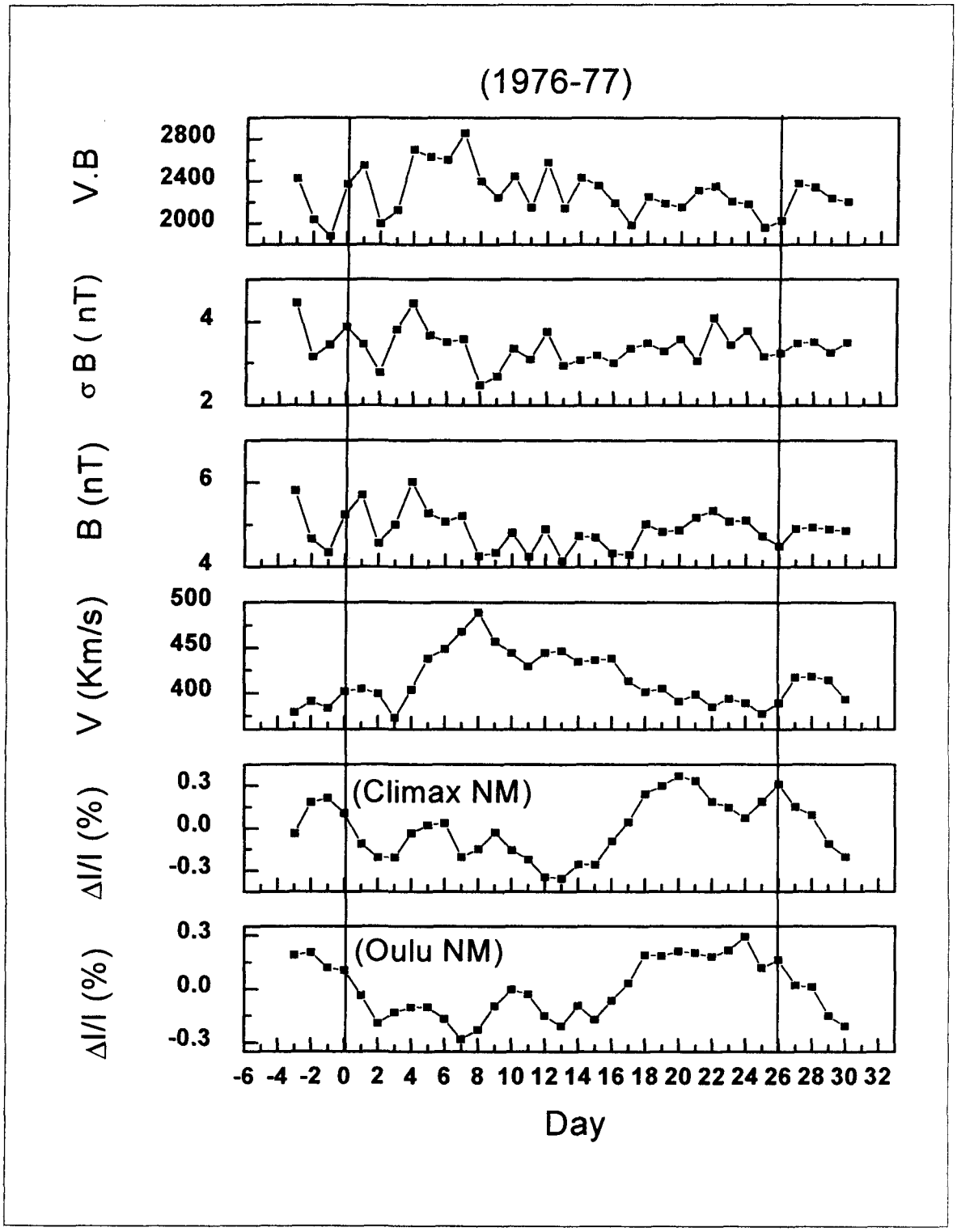

Fig. 2.1(a): Variations in daily averaged cosmic ray intensity and solar wind plasma/field parameters; zero day corresponds to the beginning date of the Carrington rotations in the minimum solar activity periods (1976-77) of a positive polarity state (A > 0).

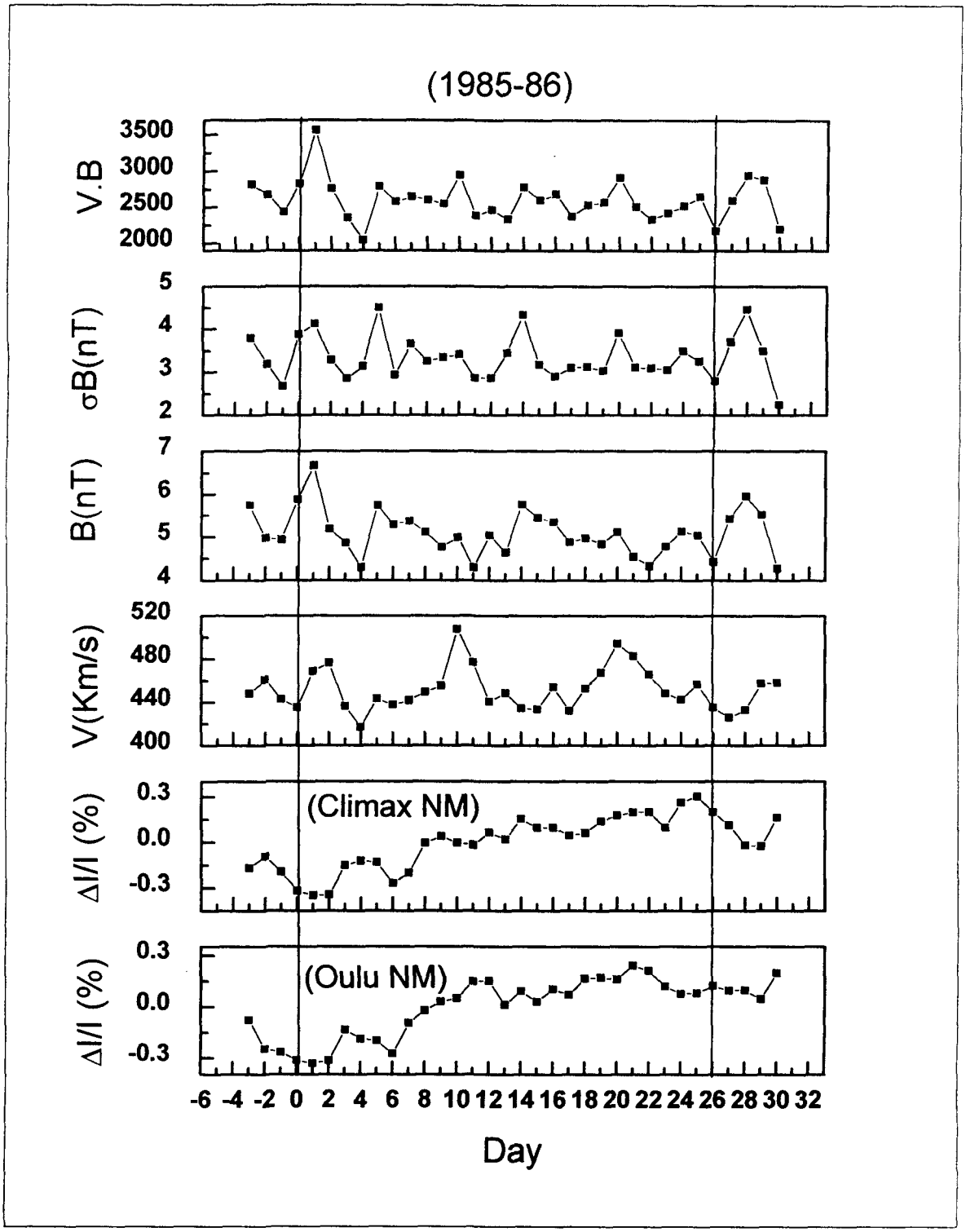

Fig. 2.1(b): Variations in daily averaged cosmic ray intensity and solar wind plasma/field parameters; zero day corresponds to the beginning date of the Carrington rotations in the minimum solar activity periods (1985-86) of a negative polarity state (A < 0).

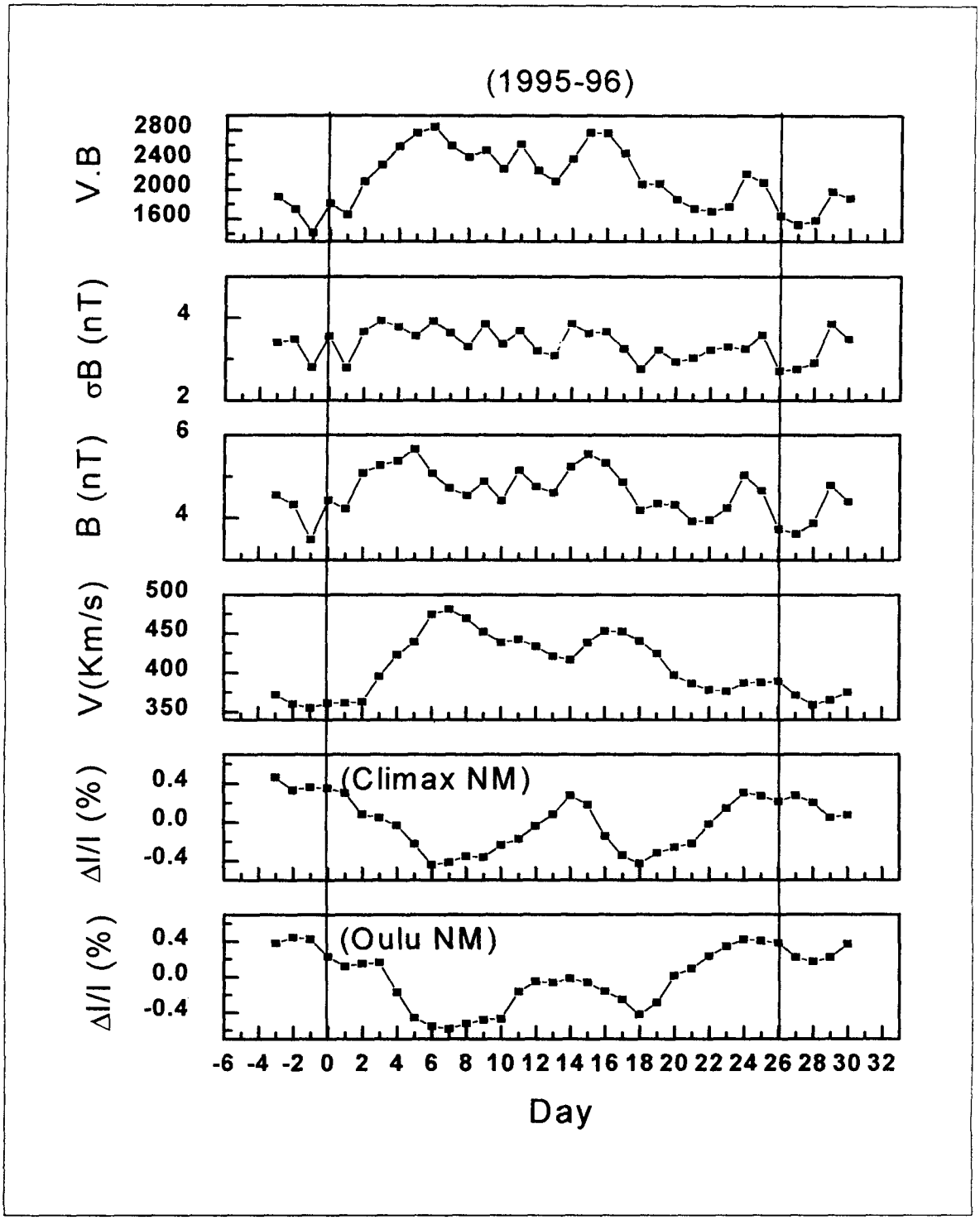

Fig. 2.1(c): Variations in daily averaged cosmic ray intensity and solar wind plasma/field parameters; zero day corresponds to the beginning date of the Carrington rotations in the minimum solar activity periods (1995-96) of a positive polarity state (A > 0).

variance (σB) and the product V.B, for the solar activity minimum periods of 1976-77 (A > 0), 1985-86 (A < 0) and 1995-96 (A > 0) respectively. Solar wind velocity (V) is related to convection and adiabatic deceleration processes contributing to GCR modulation in the heliosphere; B (and σB) is related to diffusion (scattering) of particles; gradient and curvature drift is a process of modulation that depends on solar magnetic polarity (A < 0, A > 0).

Comparison of Figs. 2.1(a), 2.l(b) and 2.1(c) show that the GCR intensity oscillates during the course of Carrington rotation, that the intensity depression is larger during A > 0 than A < 0, that the intensity oscillations do not closely follow the variation in the solar wind parameters V, B, σB and V.B in A < 0 epoch, that the solar wind velocity, at least, closely follows the intensity oscillations during the course of Carrington rotation in A > 0 epoch.

Table-1: Amplitudes of oscillations in GCR intensity and solar wind parameters during minimum periods 1976-77 (A > 0), 1985-86 (A < 0) and 1995-96 (A > 0)

Periods	**δI (Oulú)**	**δI (Climax)**	**δV**	**δB**	**$\delta(\sigma B)$**	**δ(V.B)**
1976-77	0.576	0.725	116.0	1.86	1.97	892.93
1985-86	0.573	0.651	90.8	2.37	1.64	1518.06
1995-96	1.005	0.791	119.4	1.93	1.23	1210.32

Average amplitudes of oscillations obtained from the superposed epoch plots (Fig. 2.1a, b, c) of GCR intensity and solar wind parameters, and their comparison (Table-1) shows no systematic relation between the amplitudes of average oscillations of GCR and solar wind parameters during different minimum periods.

The role of solar wind speed in corotating decreases has been the focus of special attentions since long. For example, Iucci et al. (1979) observed that maximum depression in cosmic ray density was correlated with the maximum speed inside the solar wind stream and with the magnitude of the increase in solar wind speed. Richardson et al. (1996) also observed similar relationship with a weak positive correlation. Richardson (2004) examined the relationship between maximum depression in GCR and maximum solar wind velocity for the high speed streams separately during A > 0 and A < 0 epoch. He found a weak correlation during both the epochs; however correlation between the two is better in A > 0 epochs compared to A

< 0 epoch. Relationship between the depression in GCR intensity and solar wind velocity during the course of Carrington rotation has been studied particularly in low solar activity conditions by Gupta and Badruddin (2005). Their results also show better correlation between GCR intensity and solar wind velocity during A > 0 epoch.

Table-2: Correlation coefficients between GCR intensity and solar wind parameters during minimum periods

Periods	I Vs. V	I Vs. B	I Vs. σB	I Vs. (V.B)
1976-77	-0.66	0.18	-0.27	-0.39
1985-86	0.20	-0.44	-0.22	-0.32
1995-96	-0.89	-0.40	-0.25	-0.72

Linear regression analyses between day-to-day values of average GCR intensity and solar wind parameters, plotted in Fig. 2.1(a, b, c), have also been done and correlation coefficients between GCR intensity and different solar wind parameters have been obtained. The values of correlation coefficients are given in Table-2.

It is found that the correlation coefficient between GCR intensity (I) and solar wind velocity (V) is good only in solar minimum periods 1976-77 and 1995-96, when A > 0, but not in 1985-86 when polarity state is opposite (A < 0). To show this result more clearly, scatter plots along with best-fit line (represented by I = C + mV linear equation), between averaged GCR intensity and solar wind speed during the course of Carrington rotation have been shown in Fig. 2.2 for the minimum periods 1976-77, 1985-86 and 1995-96. The best-fit values of the intensity change with velocity (m), intercept (C) and correlation coefficient (R) in different minimum periods are given in respective-figure.

It will be interesting to see whether this result suggest that (a) the cosmic ray response to solar wind speed variations is reduced in A < 0 minimum (Richardson et al., 1999), or (b) some other process/effect "obscures" the response of solar wind velocity in A < 0 epochs.

Superposed epoch plots are very useful for the study of average response of one type of phenomena activity over the other. However, simultaneous plots of recurrent parameters during individual events under study is expected to provide additional support to the conclusion drawn on the basis of superposed epoch analysis and more direct representation of one to one correspondence between them. Thus, we

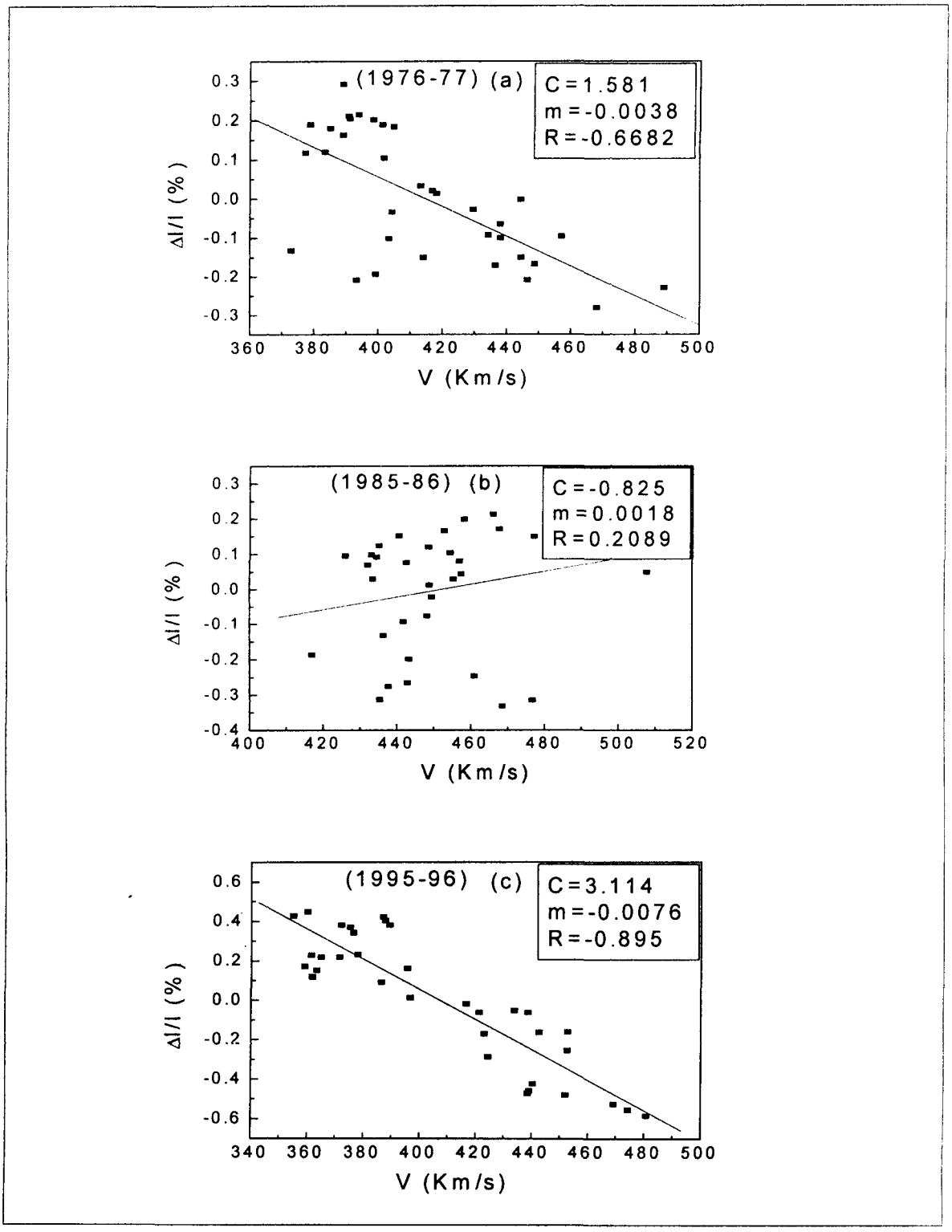

Fig. 2.2: Relationship between change in cosmic ray intensity and solar wind velocity during the course of Carrington rotation in the solar minimum periods, 1976-77, 1985-86 and 1995-96.

have plotted graphs (Fig. 2.3) showing variations in cosmic ray intensity (I), solar wind velocity (V), interplanetary magnetic field (B), its variance (σB) and the product V.B during three selected Carrington rotations, one from each minimum activity periods 1976-77, 1985-86 and 1995-96. Fig. 2.3(a) shows simultaneous variations in GCR intensity and various parameters of the solar wind during Carrington rotation number 1646 (September 13 - October 09, 1976). Similar plots of variations during Carrington rotations 1765 (August 03 - August 29, 1985) and 1909 (May 05 – May 31, 1996) are shown in Figs 2.3(b) and 2.3(c) respectively. Conclusions drawn from average plots shown in Fig. 2.1(a), 2.1(b) and 2.1(c) are well documented by individual rotation plots shown in Figs 2.3(a), 2.3(b) and 2.3(c) respectively. That is, these three plots during individual Carrington rotation show more clearly the CGR oscillations and solar wind plasma and field variations in conformity with superposed epoch plots of corresponding epochs.

The onset of recurrent modulation has been associated with various structures formed in interplanetary space, especially in the studied based on daily average neutron monitor data at earth. These structures include stream leading edges, magnetic sector boundaries (i.e. HCS), enhancement in magnetic field strength and turbulence inside the corotating structures (e.g., see Iucci et al., 1979; Scholar et al., 1979; Duggal et al., 1981). Use of high resolution (hourly) neutron monitor data (Badruddin, 1997) and high resolution guard data (Richardson et al., 1996) led these authors to conclude that recurrent modulation at 1 AU typically commence at the leading edge of the high speed stream, or at the enhancement in field turbulence in interaction region which often occurs at the stream leading edge. Cosmic ray density also tends to be anticorrelated with the solar wind speed suggesting that increased cosmic ray convection plays a major role in the production of recurrent cosmic ray depression, with the enhanced turbulence following the interface also contributing.

Solar/heliospheric magnetic field polarity effects in recurrent modulation have been studies (Richardson et al., 1999; Reames and Ng, 2001; Singh and Badruddin, 2005; Gupta and Badruddin, 2005) and modeled (Kota and Jokipii, 2001; Burger and Hitge, 2004) in recent years. Spacecraft and neutron monitor observations show that recurrent modulations are significantly larger in $A > 0$ epochs in spite of the fact that high speed streams and corotating interaction regions are not necessarily stronger in positive polarity epoch (Heber and Burger; 1999, Richardson et al., 1999). Solar

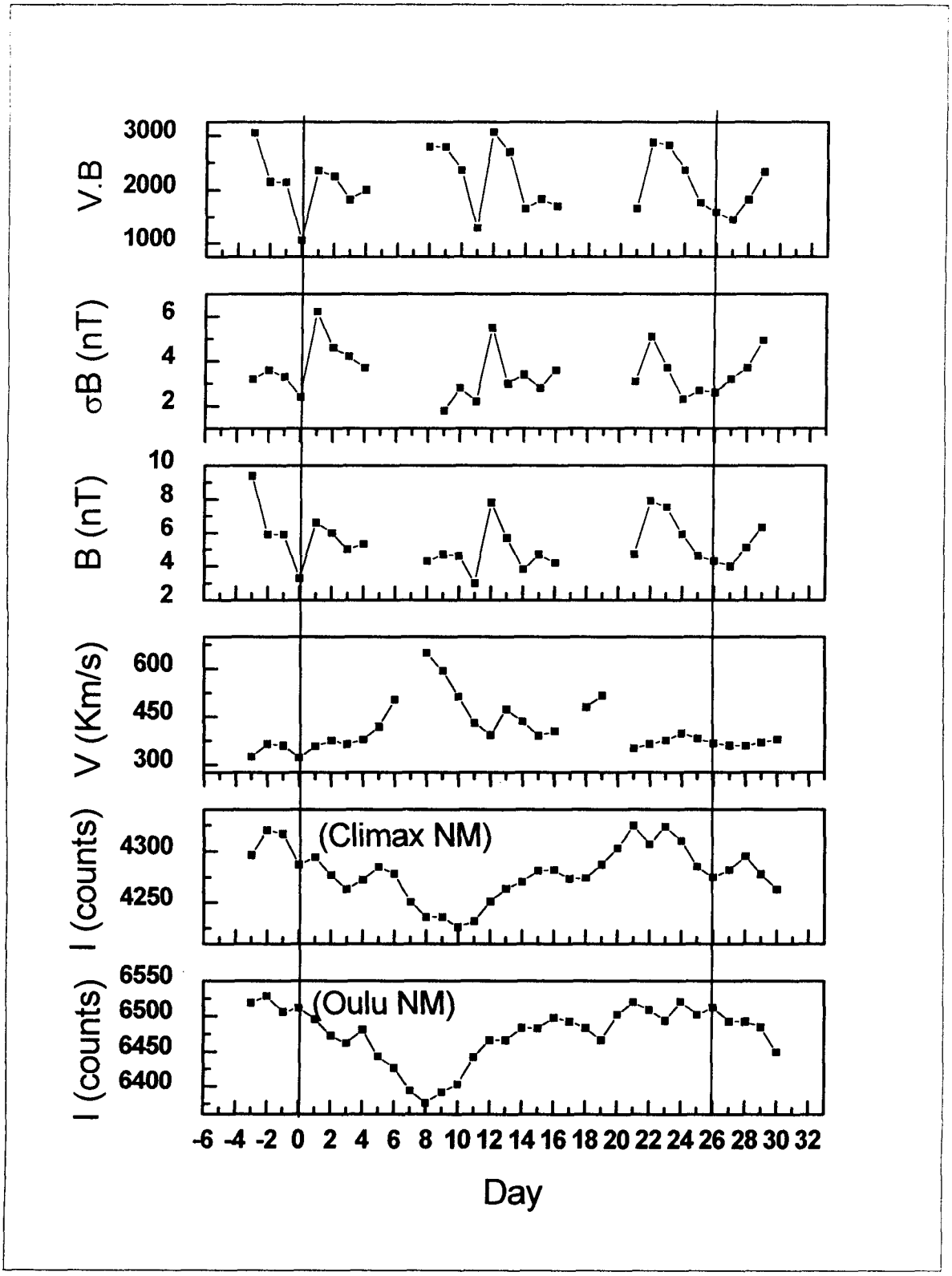

Fig. 2.3(a): Cosmic ray intensity and solar wind plasma/field variations during Carrington rotation 1646; start date (zero day), 13 September 1976.

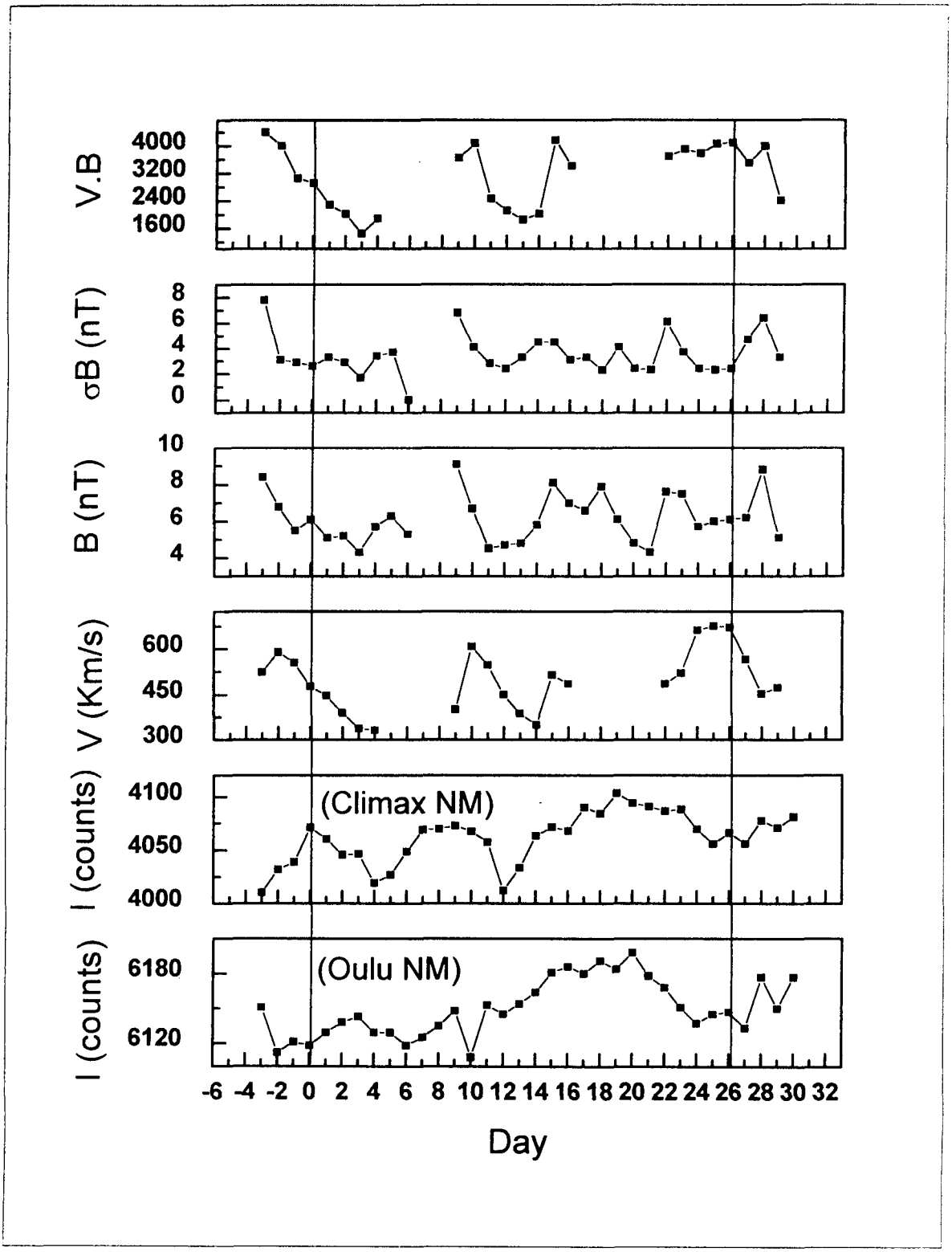

Fig. 2.3(b): Cosmic ray intensity and solar wind plasma/field variations during Carrington rotation 1765; start date (zero day), 3 August 1985.

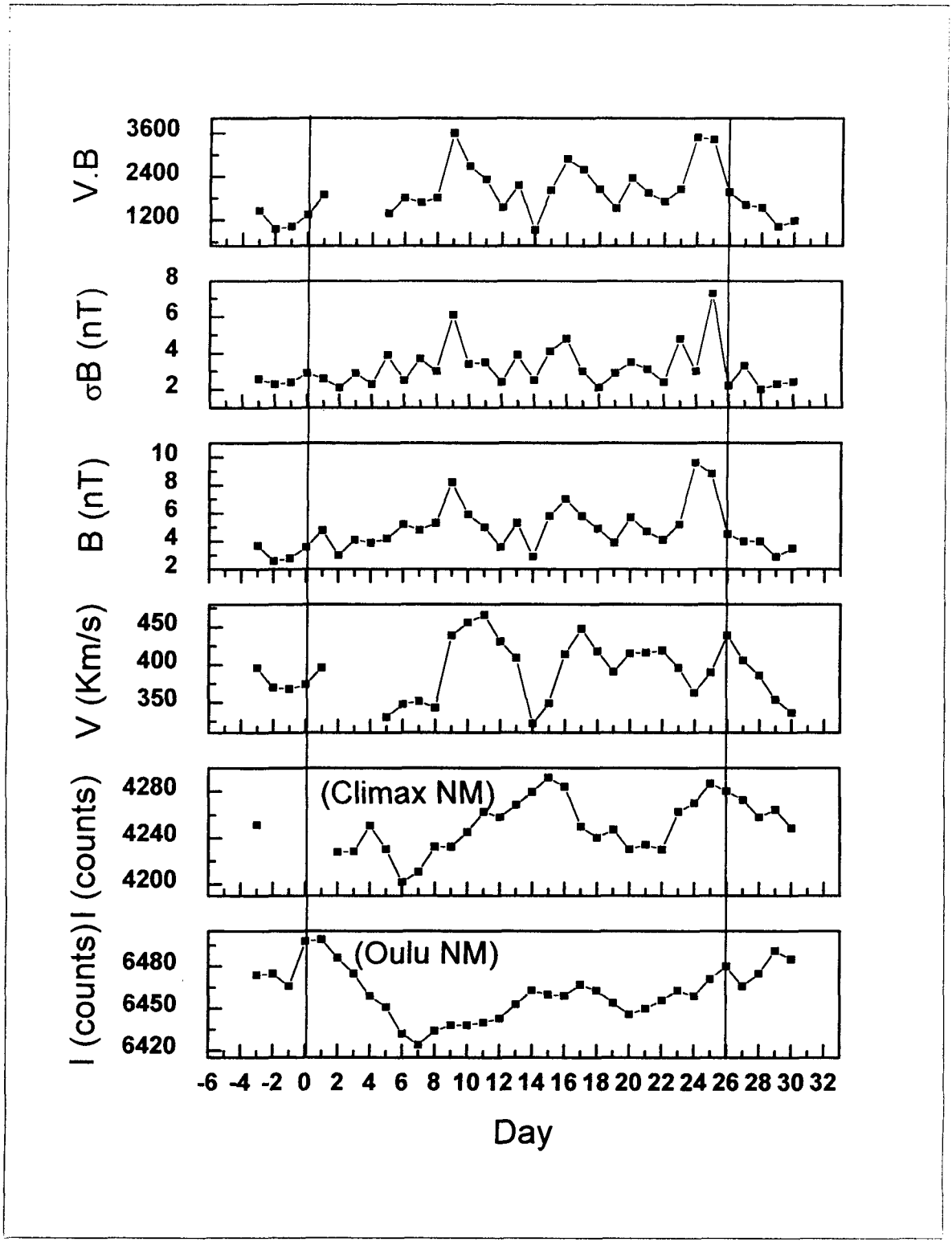

Fig. 2.3(c): Cosmic ray intensity and solar wind plasma/field variations during Carrington rotation 1909; start date (zero day), 5 May 1996.

polarity dependent recurrent modulations might be expected if there is an enhanced particle scattering at low latitudes due to corotating interaction regions (Kota and Jokipii, 1991). However, on would then expect stronger modulation in A < 0 epoch (when cosmic ray particles enter the heliosphere along the equatorial regions) than in A > 0 (when these particles enter over the poles) (Mckibben et al., 1999). But this is opposite to that what what is actually observed. Kota and Jokipii (2001) later considered a southward displaced HCS in their simulation and obtained results, which are at lest in qualitative agreement to those actually observed. Burger and Hitge (2004) investigated polarity dependent effects in the recurrent intensity variations after developing a Fisk - Parker hybrid magnetic field. Their results show polarity dependent effects and indicate increases with increase in tilt angle. that drifts may be important for corotaing modulations. However, if effects due to local diffusion were predominant, then no polarity dependence would be expected. In this case, there is a possibility that particle transport parameters have a solar field dependence (e.g. Chen and Bieber, 1993), such as to enhance the effect of cosmic ray convection in A > 0 epochs (Richardson et al., 1999).

Since tilt angle of the HCS is an important parameter in drift models of cosmic ray modulation, we have studied the relationship between tilt angle and cosmic ray oscillations during corresponding rotations. For this purpose, we have plotted the amplitudes of GCR oscillations versus the tilt angle in individual Carrington rotations (http://soi.stanford.edu/~wso/Tilts.html). The scatter plot, best fit linear curve, along with the value obtained for the correlation coefficient (R), density gradient with respect to tilt angle of HCS (m) and intercept (C) is shown in Fig. 2.4 for the periods 1976-77, 1985-86 and 1995-96. Since correlation coefficient is small, we could not draw any definite conclusion about the density gradients during different minima; however, we infer that there is some evidence that GCR oscillation during Carrington rotations

Richardson et al. (1999), Gil et al. (2005) have found that the amplitudes of recurrent variations in GCR intensity are larger for A > 0 than for A < 0 period of solar magnetic cycle. Gil et al. (2005) observed a positive but insignificant gradient in recurrent modulation of GCR intensity with tilt angle in both the epochs, and concluded that amplitude of 27-day variation of GCR intensity does not depend on the tilt angle of the HCS, similar to the conclusions of Gil and Alania (2001).

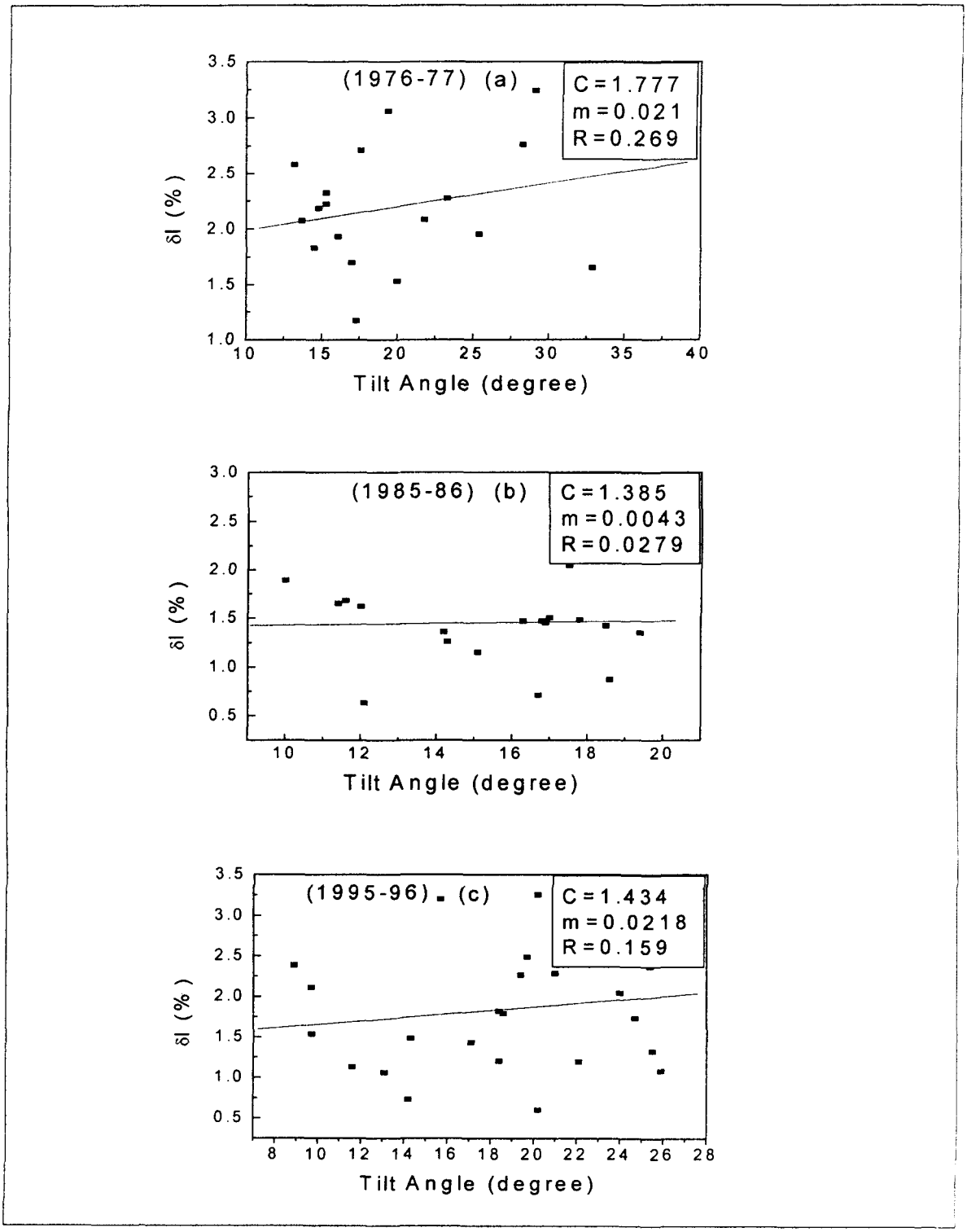

Fig. 2.4: Amplitudes of oscillations in GCR intensity during different Carrington rotations versus relationship with tilt angle of HCS during three solar minima (1976-77, 1985-86 and 1995-96).

The relationship between the amplitude of recurrent oscillations and heliolatitude gradient was studied by Zhang (1997) and Paizis et al. (1999) utilizing the data of Ulysses spacecraft. Zhang (1997) discovered from Ulysses observations in A> 0 epoch that there exists a linear relationship between the magnitude of latitude gradient and the amplitude of 26-day recurrent modulation in the fluxes of GCR. The linear relationship holds for recurrent modulation observed in the inner heliosphere at all latitude, and apparently, independent of particle energy and nuclear species. His investigation with Voyager and IMP-8 in the A< 0 epoch also displayed this linear relationship even though the latitude gradient had a negative sign. His investigations suggest that there is a common, dominant modulation mechanism controlling both the global latitudinal distribution and 26-day modulation of cosmic ray flux.

Earth based detectors (e.g. neutron monitors) used for the measurement of GCR intensity show a variation of a period of one day (diurnal variation) whose amplitude is ~0.5% due to the rotation of earth. Since corotating decreases observed by neutron monitors are usually not very large (≤ 2 - 3 %), use of daily averaged data for the study of corotating decreases averages out the effect of daily variations. Thus, it is better to use daily averaged GCR intensity data of ground based detectors if one is interested only in the study of behavior of corotating decreases, e.g. during different solar activity and solar magnetic condition. However, if one is interested in studying the role of various fine structures responsible for corotating decreases and their relative effectiveness in producing such modulations, it is better to use data with higher resolution (e.g. ~1 hour). For example, the onset and amplitude of corotating decreases may be associated with increase in solar wind speed, sector boundary (HCS) crossings, magnetic field enhancements, larger field fluctuations (e.g. see Richardson et al., 1996, 1999; Badruddin, 1997; Richardson, 2004). In order to study the relative importance and role of these parameters, we have used hourly data of GCR intensity observed by neutron monitors, solar wind velocity (V), heliosphere magnetic field strength (B) and it's variance (σB).

In the inner heliosphere, two basic kinds of recurrent phenomenon in the solar wind and interplanetary magnetic fields have been found. One is the heliospheric current sheet that is usually tilted from the solar equator. As the sun rotates, the heliomagnetic latitude at the spacecraft, which is proportional to it's distance to the current sheet, changes periodically. The other recurrent phenomenon is the corotating

interaction region, which is the result of compression between slow and fast solar wind streams. Since the slow wind mainly originates from the equatorial zone and the fast wind streams come from polar coronal holes, a persistent equatorial extension of a polar coronal hole will produce a series of corotating interaction regions as observed by an interplanetary spacecraft. Both heliospheric current sheet and corotating interaction regions are expected to modulate cosmic rays up to same degree of latitude; thus both produce 26-day recurrent variations in the cosmic ray flux (Simnett et al., 1998). However, it is interesting to know whether the primary cause of recurrent cosmic ray modulation is tilted HCS or corotating interaction regions. Although the effects of HCS and CIR can not be easily distinguished, there are evidence supporting one or the other and more studies are needed to resolve this question.

Since high speed corotating streams are more prominently observed during a period of 2 -3 years before to the activity minimum, we have studied the modulation during Carrington rotation periods separately during two periods, 1983-84 ($A < 0$) and 1993-94 ($A > 0$); both periods lie before the minimum activity periods. In Fig. 2.5(a), superposed epochs results of GCR intensity, solar wind velocity, IMF strength and its variance with respect to Carrington rotation for the period 1983-84 are plotted. Results of similar analysis for the period 1993-94 are shown in Fig. 2.5(b). Comparison of Fig. 2.5(a) and 2.5(b) shows that the amplitude of oscillations in GCR intensity during the two periods are almost same, (see also Table-3) although the average time profiles in the two periods are different. Further, the amplitudes of oscillations in B, σB and V.B are also nearly same in two periods, but the amplitude oscillation in solar wind velocity (δV) is higher in 1983-84 than in 1993-94 (Table-3).

Table-3: Amplitudes of average oscillations during Carrington rotation in GCR intensity and solar wind parameters in low solar periods of declining phase of solar cycles

Periods	**δI (Oulu)**	**δI (Climax)**	**δV**	**δB**	**$\delta(\sigma B)$**	**δ(V.B)**
1983-84	1.058	1.140	197.2	3.64	4.87	2606.54
1993-94	1.030	1.100	156.9	4.52	4.03	2579.16

Correlation coefficients between GCR intensity and various interplanetary parameters during 1983-84 and 1993-94 have been calculated; they are given in Table-4. It is interesting to note that the GCR intensity is better correlated with day-to-day variations

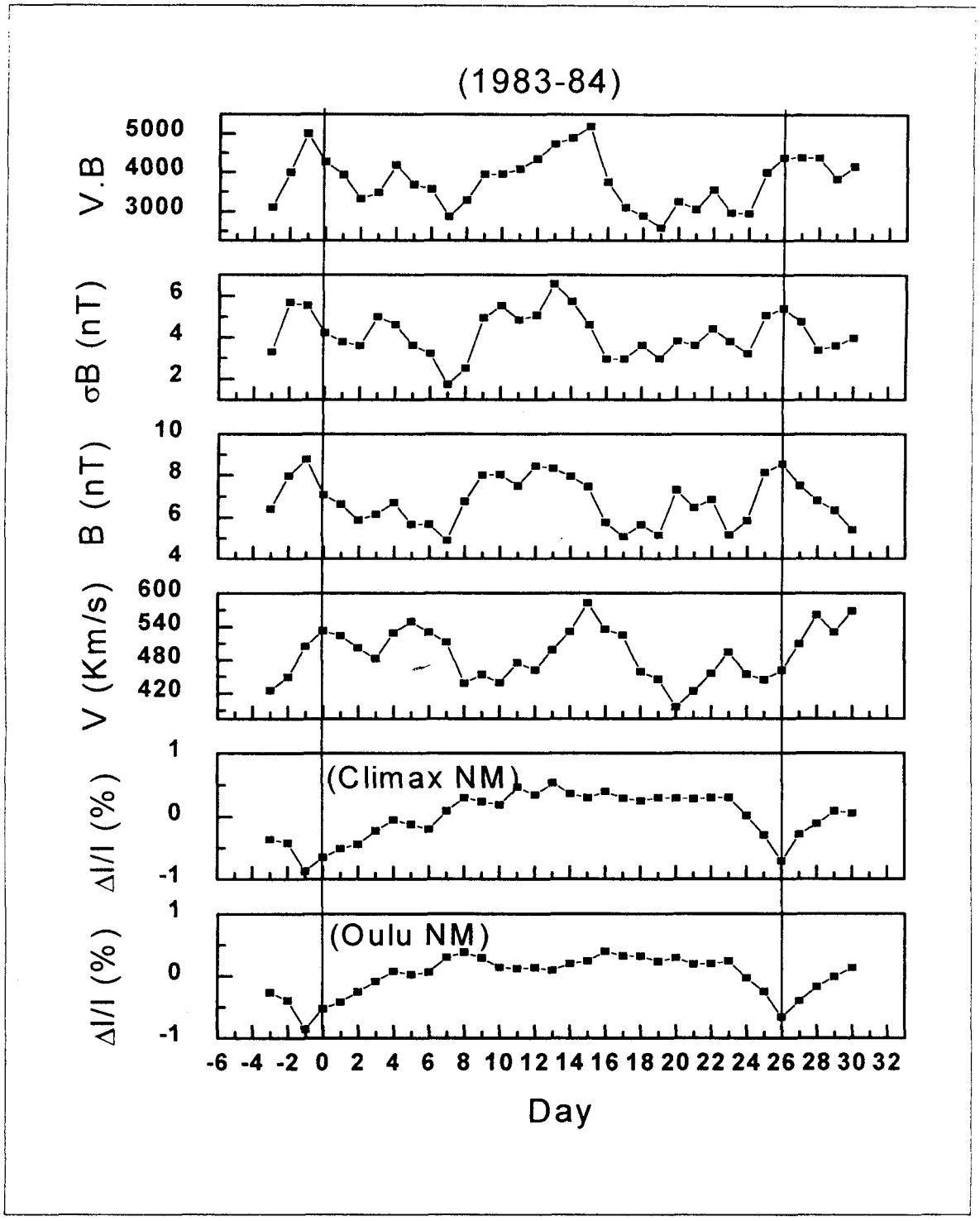

Fig. 2.5(a): Superposed epoch analysis results showing the variations in GCR intensity and solar wind parameters in the course of Carrington rotations during negative polarity state and a period of low activity in the decreasing phase (1983-84) of a solar cycle: zero day correspond to beginning of rotations.

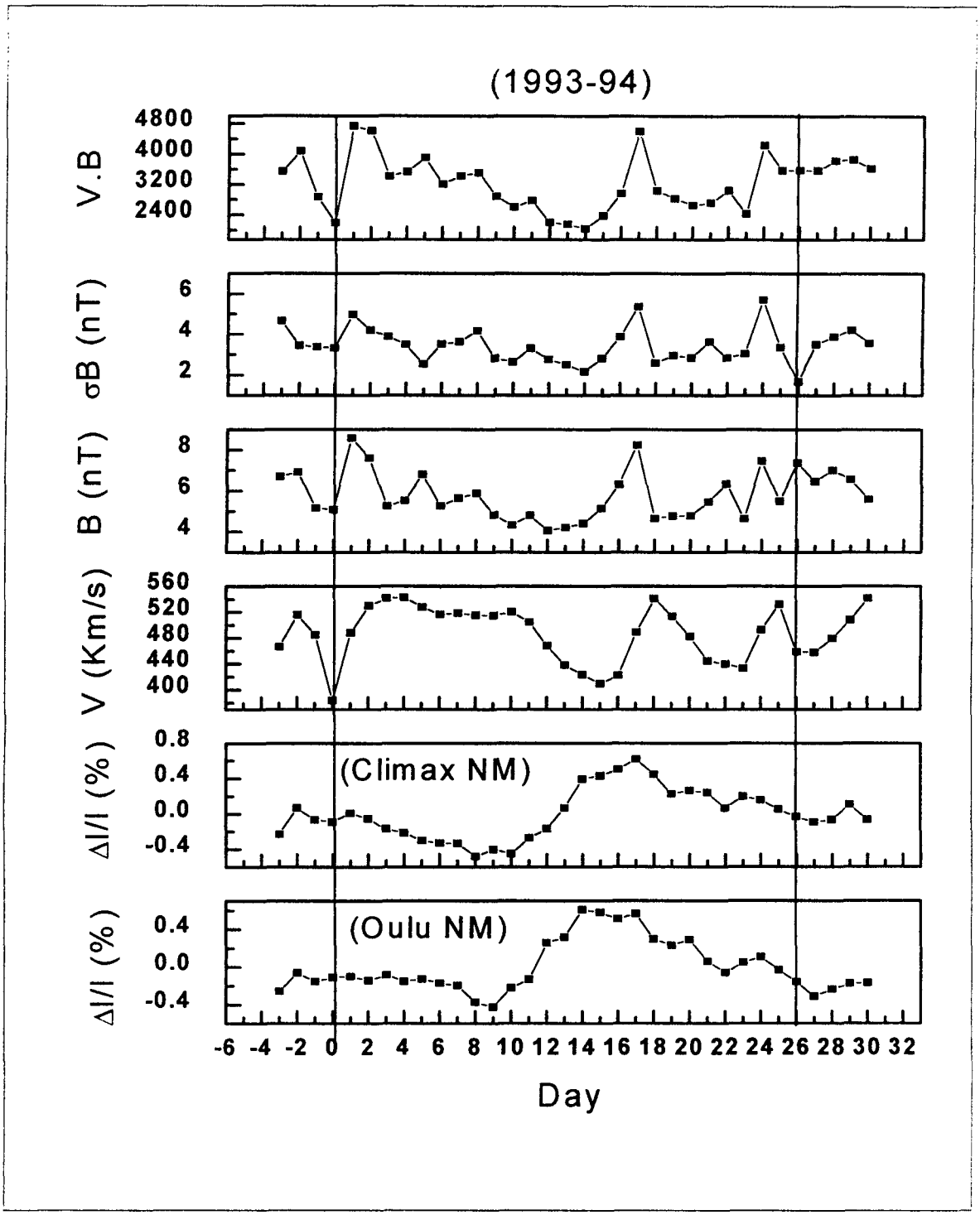

Fig. 2.5(b): Superposed epoch analysis results showing the variations in GCR intensity and solar wind parameters in the course of Carrington rotations during positive polarity state and a period of low activity in the decreasing phase (1993-94) of a solar cycle: zero day correspond to beginning of rotations.

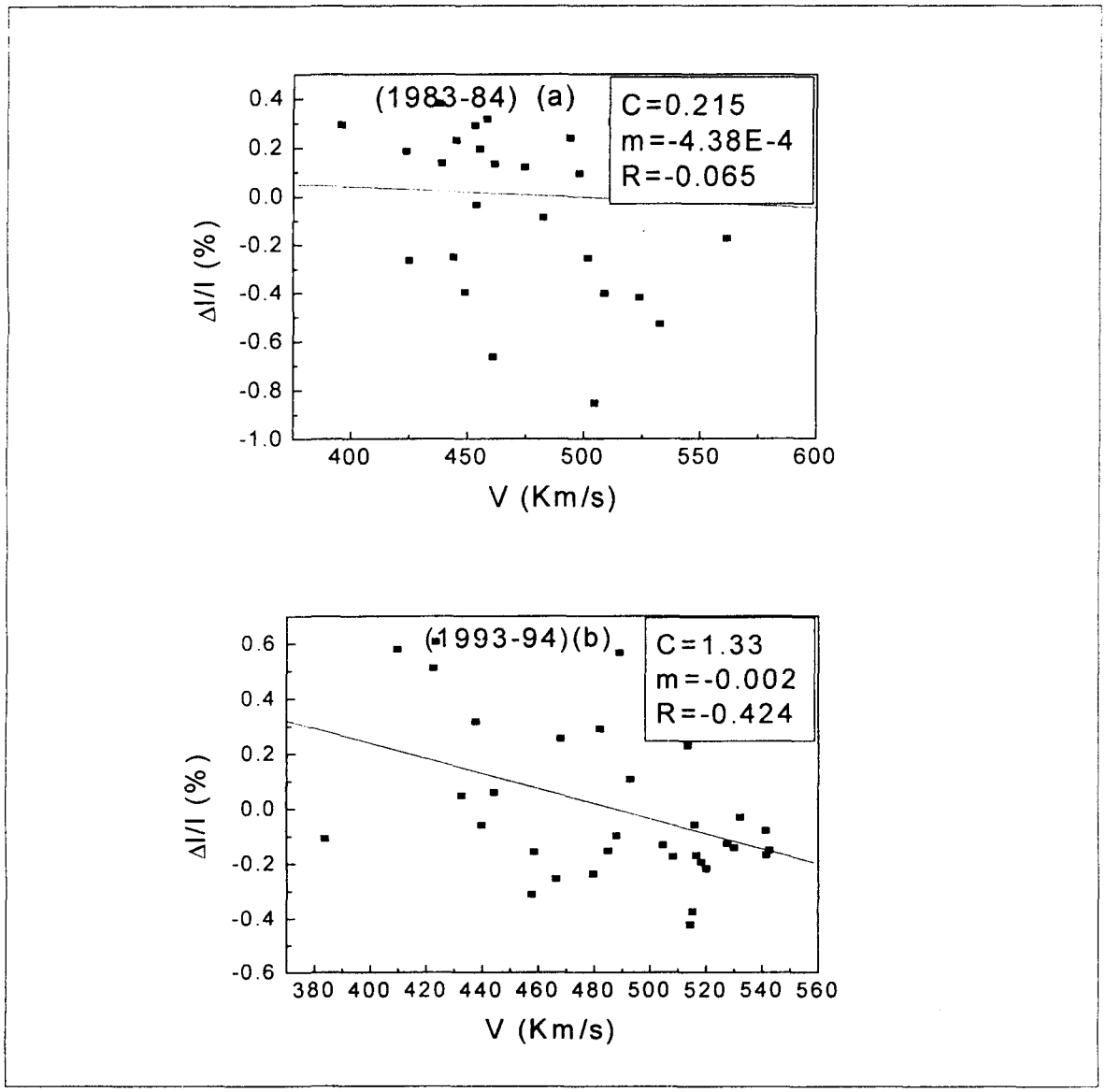

Fig. 2.6: Relationship between cosmic ray intensity and solar wind velocity during two different polarity states of the heliosphere (A < 0 and A > 0) in low solar activity conditions and during deeling phases of two different solar activity cycles.

in solar wind velocity (V) during 1993-94 (A > 0) while its correlation is better with field magnitude (B) during 1983-84 (A < 0).

Table-4: Correlation coefficients between GCR intensity and solar wind parameters during the course of Carrington rotation in two low solar activity periods in declining phase of different solar cycles

Periods	I Vs. V	I Vs. B	I Vs. σB	I Vs. (V.B)
1983-84	-0.06	-0.42	-0.37	-0.39
1993-94	-0.42	-0.17	-0.11	-0.32

Scatter plots between GCR and solar wind velocity during the two periods together with the best-fit linear curves are shown in Fig. 2.6; the value of intercept (C), slope (m) and correlation coefficient (R) are also given.

Two individual plots, one for Carrington rotation number 1754 (start date 7 October, 1984) (Fig. 2.7(a)) and other for rotation number 1885 (start date 20 July, 1994) (Fig. 2.7(b)) show the relationship between GCR intensity and solar wind parameters. The anti-correlation between GCR intensity (I) and solar wind velocity (V) apparent during the latter plot, but it is not so clearly visible in the former plot in conformity the average behavior seen during the corresponding periods.

We have calculated the amplitudes of oscillations during each rotation of periods 1983-84 and 1993-94 and did correlation analysis between amplitude of oscillations and corresponding rotation tilt angles for the periods 1983-84 and 1993-94. Scatter plot between the two quantities is shown in Fig. 2.8. Correlation coefficient (R) being very low in both the periods, we could not draw any definite conclusion about a relationship between them.

For modulation models in which the variations in heliomagnetic latitude is the primary source of the 26-day recurrent variation of GCR, one would expect that the amplitude of cosmic ray oscillations be correlated with the tilt angle of the HCS. On the other hand, if CIRs are the primary cause of recurrent cosmic ray modulation, one would expect (a) a close anti correlation with solar wind velocity; (b) in every transition from slow solar wind to fast solar wind, where CIR and magnetic field compression occur, the GCR intensity decreases rapidly and then it is followed by gradual recovery in the solar wind rarefaction region.

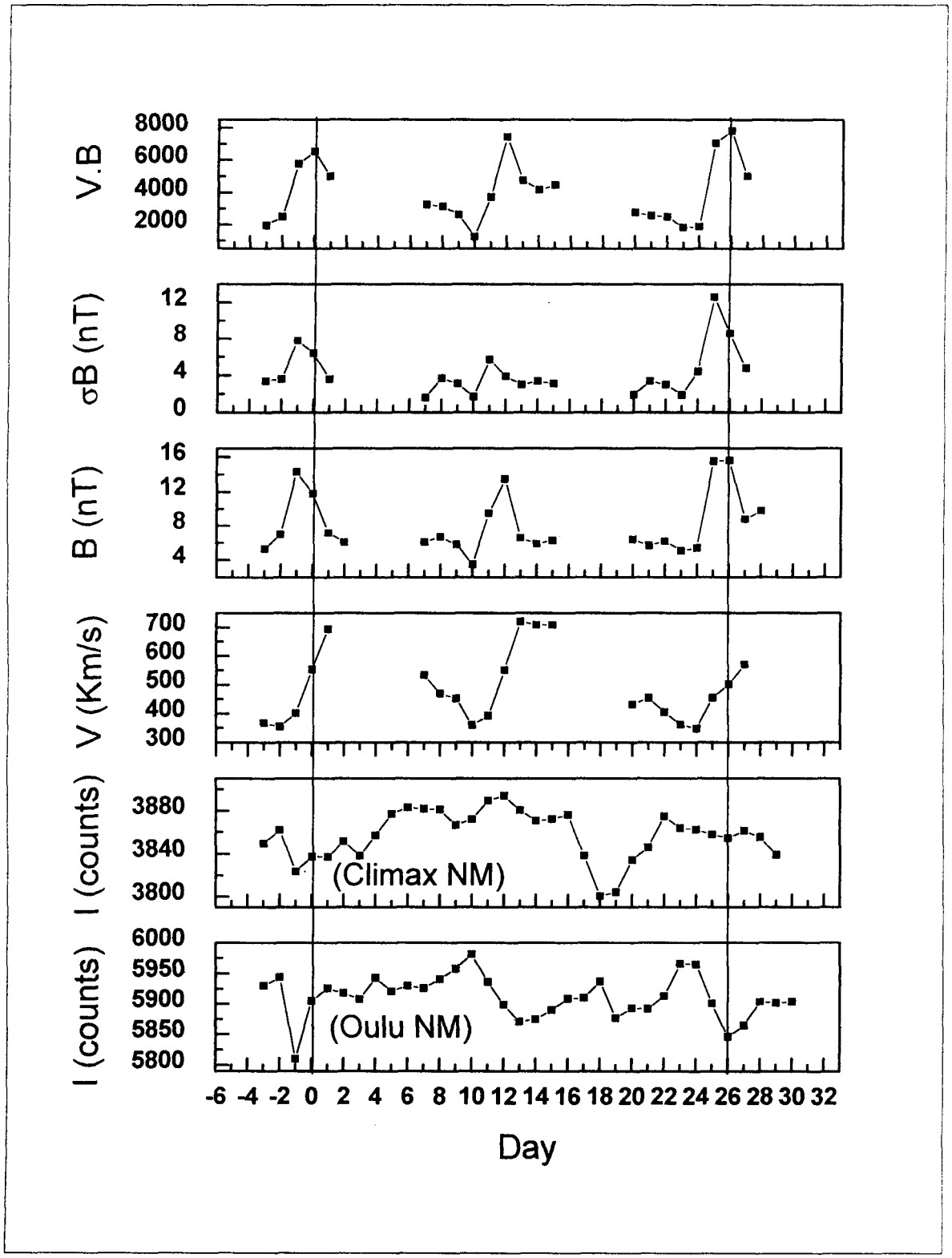

Fig. 2.7(a): Cosmic ray intensity and solar wind plasma/field variations during Carrington rotation 1754; start date (zero day), 7 October 1984.

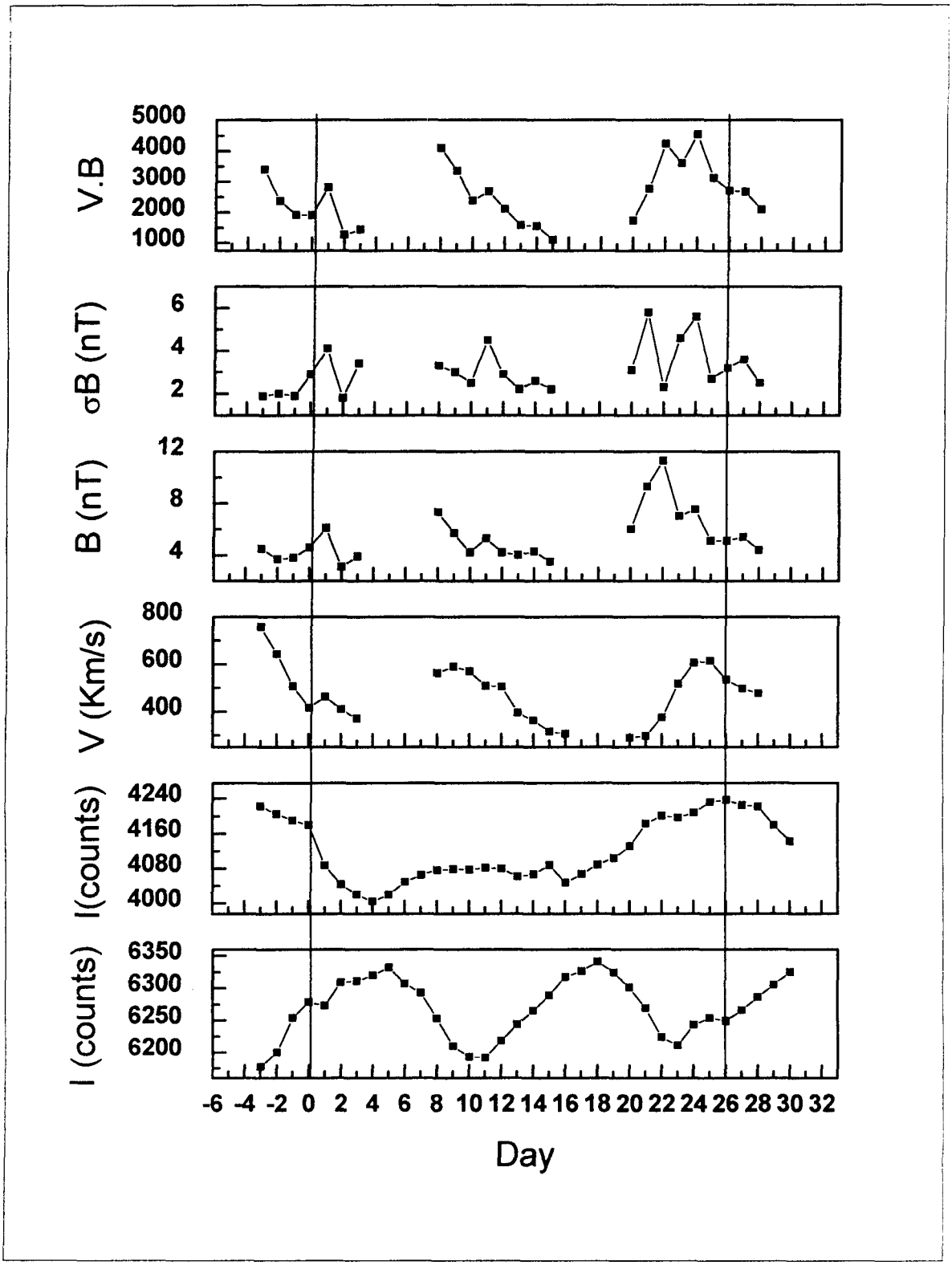

Fig. 2.7(b): Cosmic ray intensity and solar wind plasma/field variations during Carrington rotation 1885; start date (zero day), 20 July 1994.

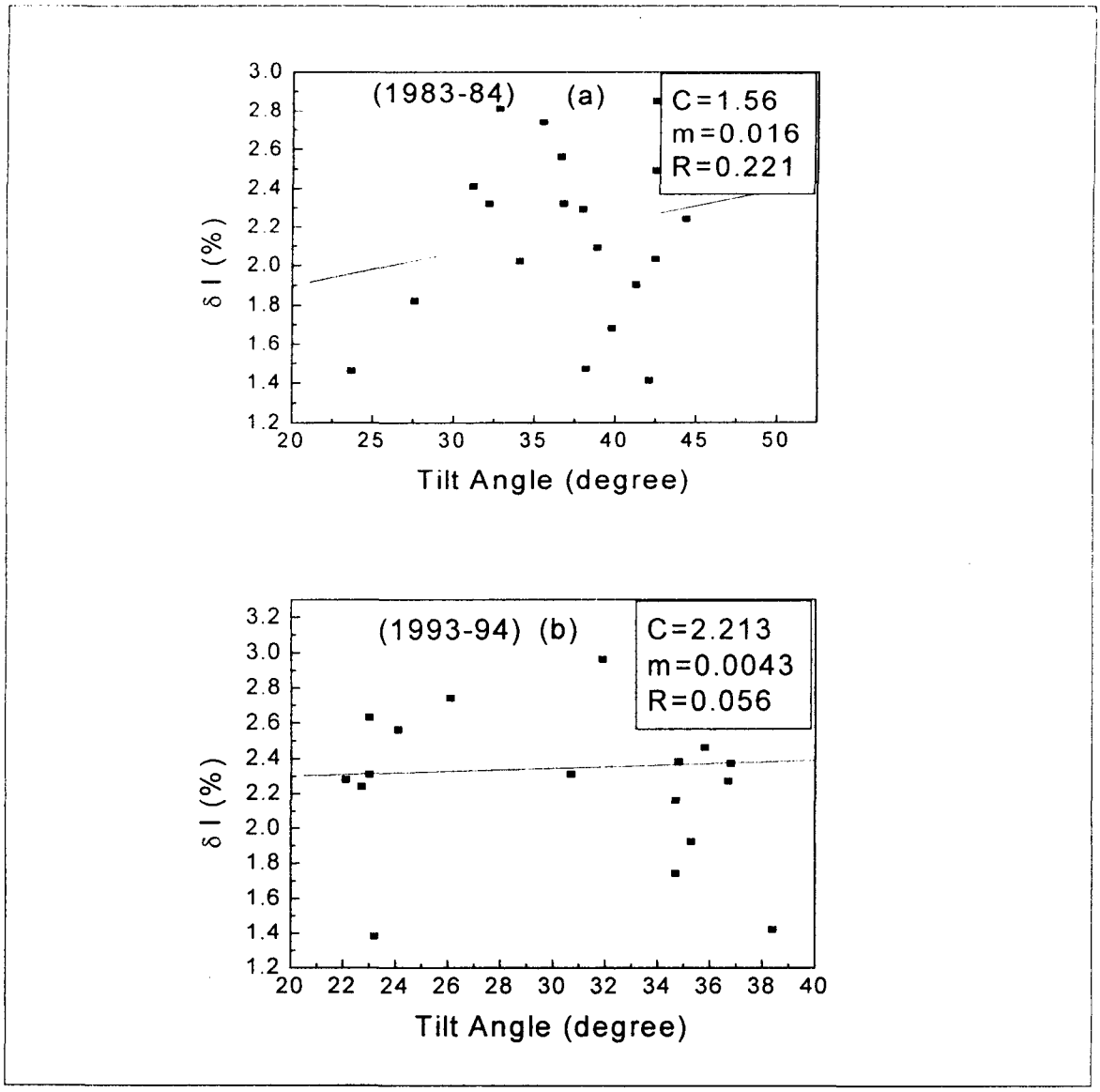

Fig. 2.8: Relationship between oscillations in GCR intensity and tilt angles during Carrington rotations in declining and low solar activity periods of two solar cycles: 1983-84 and 1993-94.

Although the analyses exclusively during solar minimum periods and during the periods when high-speed solar wind streams are prominently observed have certain advantages, the number of Carrington rotations in each group (in which GCR intensity was free from transient effects) was not large enough, e.g. during each of the three minimum periods 1976-77, 1985-86, 1995-96, and two high-stream periods 1983-84, 1993-94.

In order to increase the statistics of data we then considered the combined periods 1983-86 ($A < 0$) and 1993-96 ($A > 0$) for data analysis. Figs. 2.9(a) and 2.9(b) show the superposed epoch plots of GCR intensity and solar wind parameters during these periods of different solar polarity. Average amplitudes of GCR oscillations, solar wind velocity, IMF strength and its variance along with the product V.B obtained from these plots are given in Table-5. It is observed from Fig. 2.9(a), 2.9(b) and Table-5, that the average oscillation in GCR intensity is nearly same in two periods. As regards the oscillations in solar wind parameters, the oscillation amplitude of solar wind velocity and field magnitude is somewhat larger in 1993-96.

Table-5: Amplitudes of average oscillations obtained from superposed epoch plots of GCR intensity and solar wind parameters during two periods in different solar polarity epoch ($A < 0$ and $A > 0$)

Periods	**δI (Oulu)**	**δI (Climax)**	**δV**	**δB**	**$\delta(\sigma B)$**	**δ(V.B)**
1983-86	0.661	0.742	64.70	1.87	2.35	1317.87
1993-96	0.682	0.750	90.00	2.18	2.28	1545.89

Table-6: Correlation coefficients between GCR intensity and solar plasma/field parameters during the course of Carrington rotation

Periods	**I Vs V**	**I Vs B**	**I Vs σB**	**I Vs (V.B)**
1983-86	-0.08	-0.44	-0.32	-0.42
1993-96	-0.68	0.29	-0.02	-0.27

We did a correlation analysis of GCR intensity with average variations in V, B, σB and V.B, plotted in Fig. 2.9(a) and 2.9(b); and the correlation coefficients so obtained are tabulated in Table-6. Since solar wind velocity shows a better (anti-) correlation with GCR intensity during the course of Carrington rotations, at least during

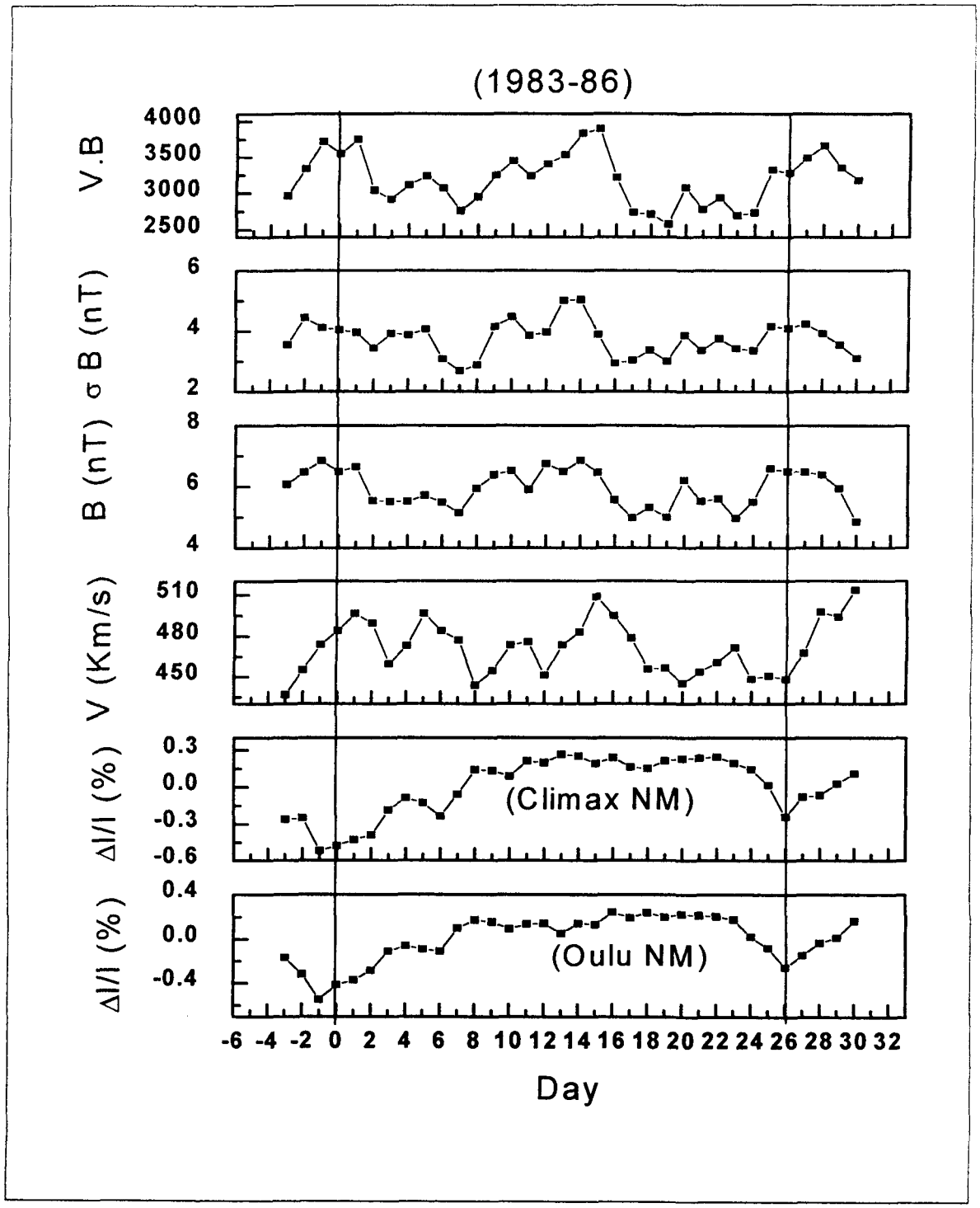

Fig. 2.9(a): Superposed epoch analysis results showing variations in cosmic ray intensity and solar plasma/field parameters with respect beginning of Carrington rotation in low activity periods (1983-86) when the polarity state of the heliosphere was in negative state ($A < 0$).

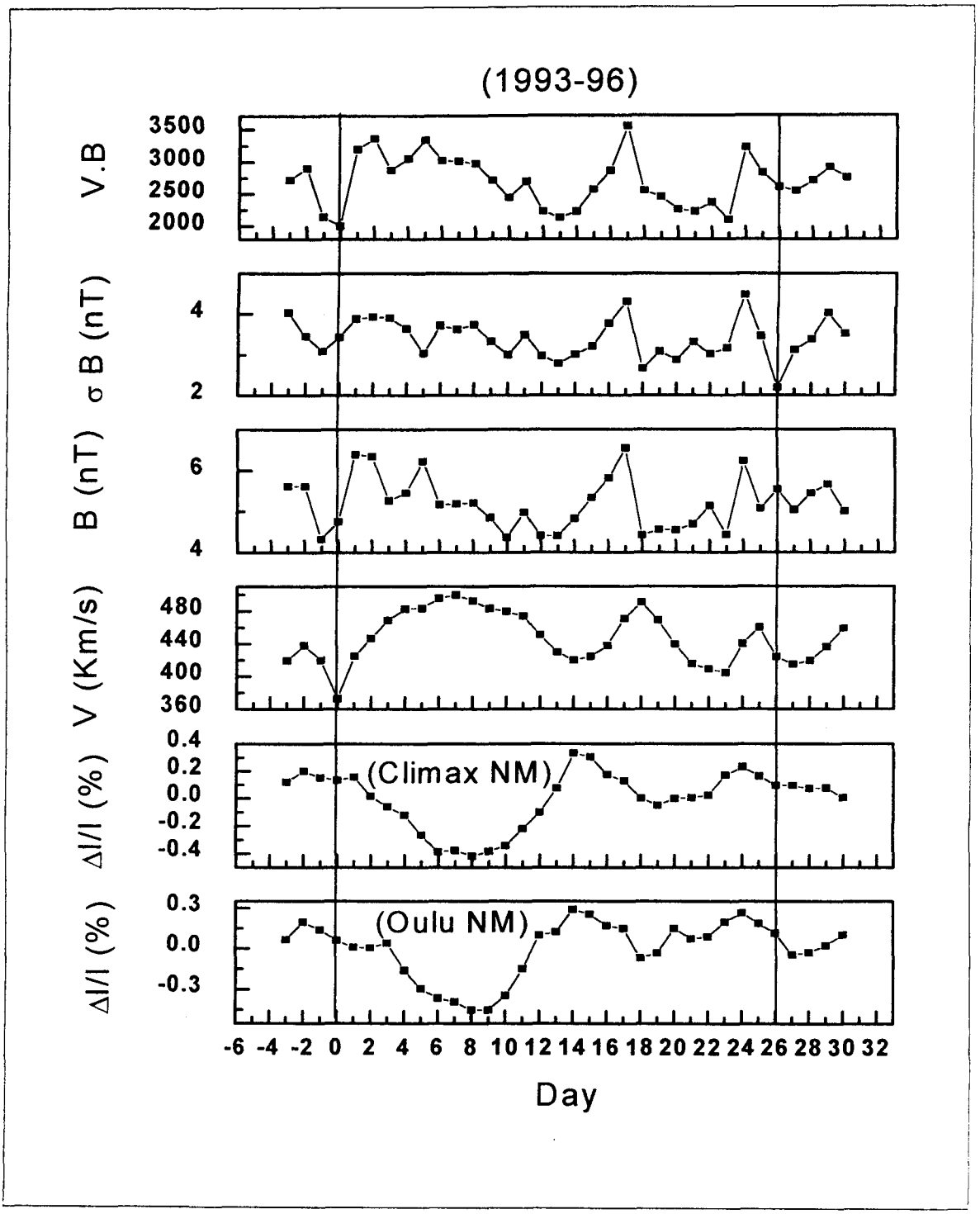

Fig. 2.9(b): Superposed epoch analysis results showing variations in cosmic ray intensity and solar plasma/field parameters with respect beginning of Carrington rotation in low activity periods (1993-96) when the polarity state of the heliosphere was in positive state (A > 0).

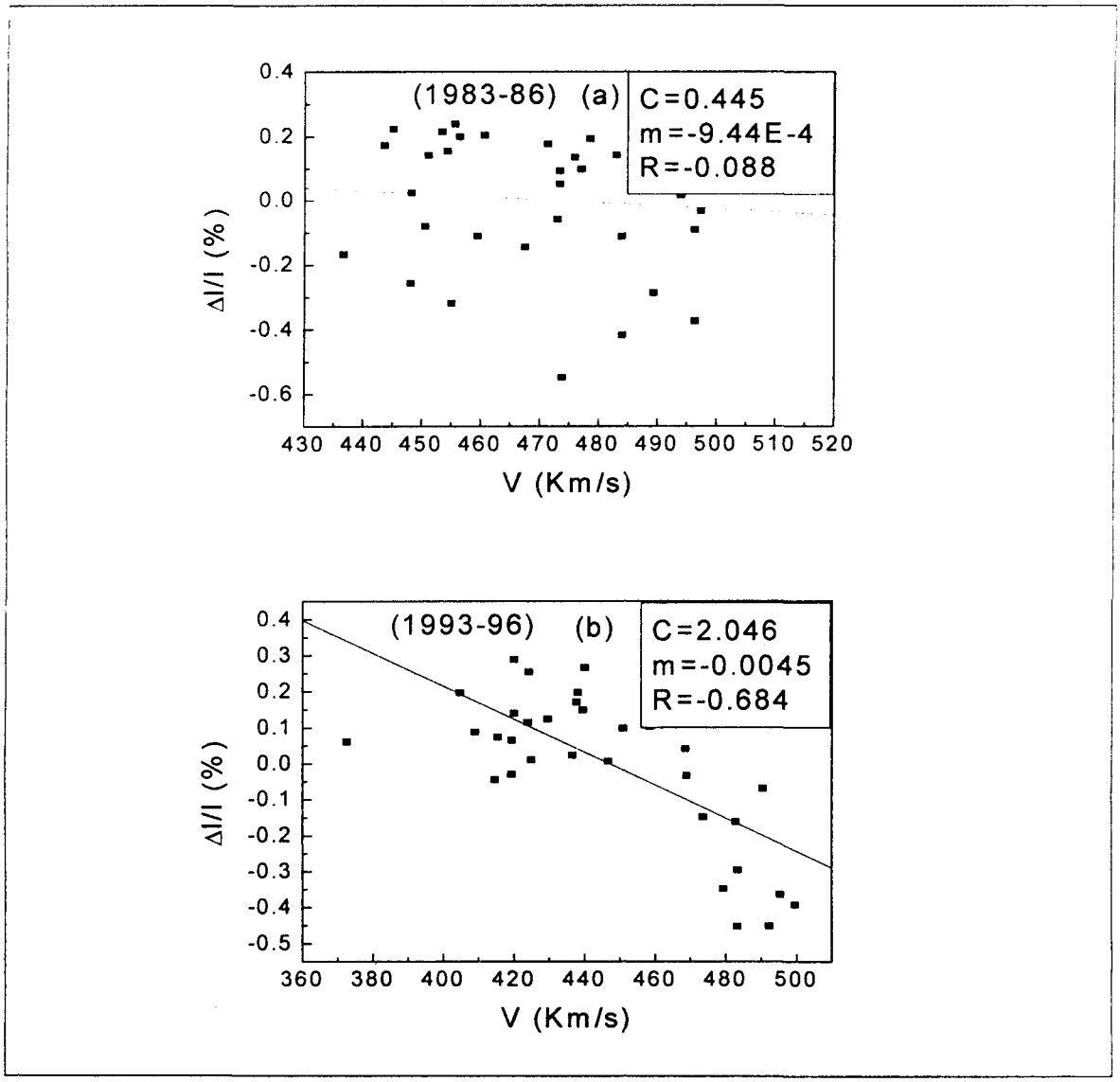

Fig. 2.10: Relation between solar wind velocity and cosmic ray intensity changes during the course of Carrington rotation (a) 1983-86 (A < 0) and (b) 1993-96 (A > 0).

A> 0 epochs, we have shown the scatter plots of solar wind velocity with GCR intensity together with the best-fit curve, intercept (C), intensity gradient with solar wind velocity (m) in Fig. 2.10. It is more clearly seen here that a good correlation exists between these two parameters only during A> 0 epoch.

Relationship between GCR oscillations in individual Carrington rotation and tilt angle of HCS has also been studied during these two periods of different polarity states of the heliosphere i.e. 1983-86 (A < 0) and 1993-96 (A > 0). This relationship along with the best-fit linear line is shown in Fig. 2.11. These two plots provide some evidence that amplitude of recurrent GCR oscillations increases with tilt angle during both the polarity epochs A > 0 and A < 0, the gradient being nearly same in both the epochs, ~ 0.03 % per degree tilt angle. From neutron monitor observations in 1975, Newkirk and Fisk (1981) found a value of about 0.04 % per degree latitudinal gradients at 5 GeV. Badruddin and Yadav (1985) also estimated the heliomagnetic latitudinal gradient and found it to be ~ 0.04 % per degree in 1974. For 1970-79 period the symmetric latitudinal gradient away for the HCS was estimated to be 0.06 % per degree (Newkirk and Fisk, 1985). The theoretical predictions, including warped current sheet yields about 0.06 % per degree (Kota and Jokipii, 1983).

Studies based on daily average GCR intensity data have an advantage, that it eliminates the fluctuations in data due to daily variations. However, the onset of corotating decrease, its correspondence with variations in solar wind parameters and its coincidence with various structures of CIRs/HCS can be better understood with the use of data of higher time resolution. In order to study the finer details of variations in GCR during the course of Carrington rotations, data of one-hour resolution were used for the superposed analysis as well as individual events analysis. Fig. 2.12(a), 2.12(b) and 2.12(c) are the superposed epoch plot of hourly data during three minimum periods (1976-77, 1985-86 and 1995-96).

Similar plot for two periods (1983-84, 1993-94) preceding solar minimum periods, when corotating high-speed streams are more frequently observed, are plotted in Fig. 2.13(a) and 2.13(b). Two plots for the periods 1983-86 and 1993-96 during low activity periods of different polarity are shown in Fig. 2.14(a) and 2.14(b). These plots show finer details of fluctuations in cosmic ray intensity and various solar wind parameters during the course of Carrington rotations in different solar and magnetic conditions.

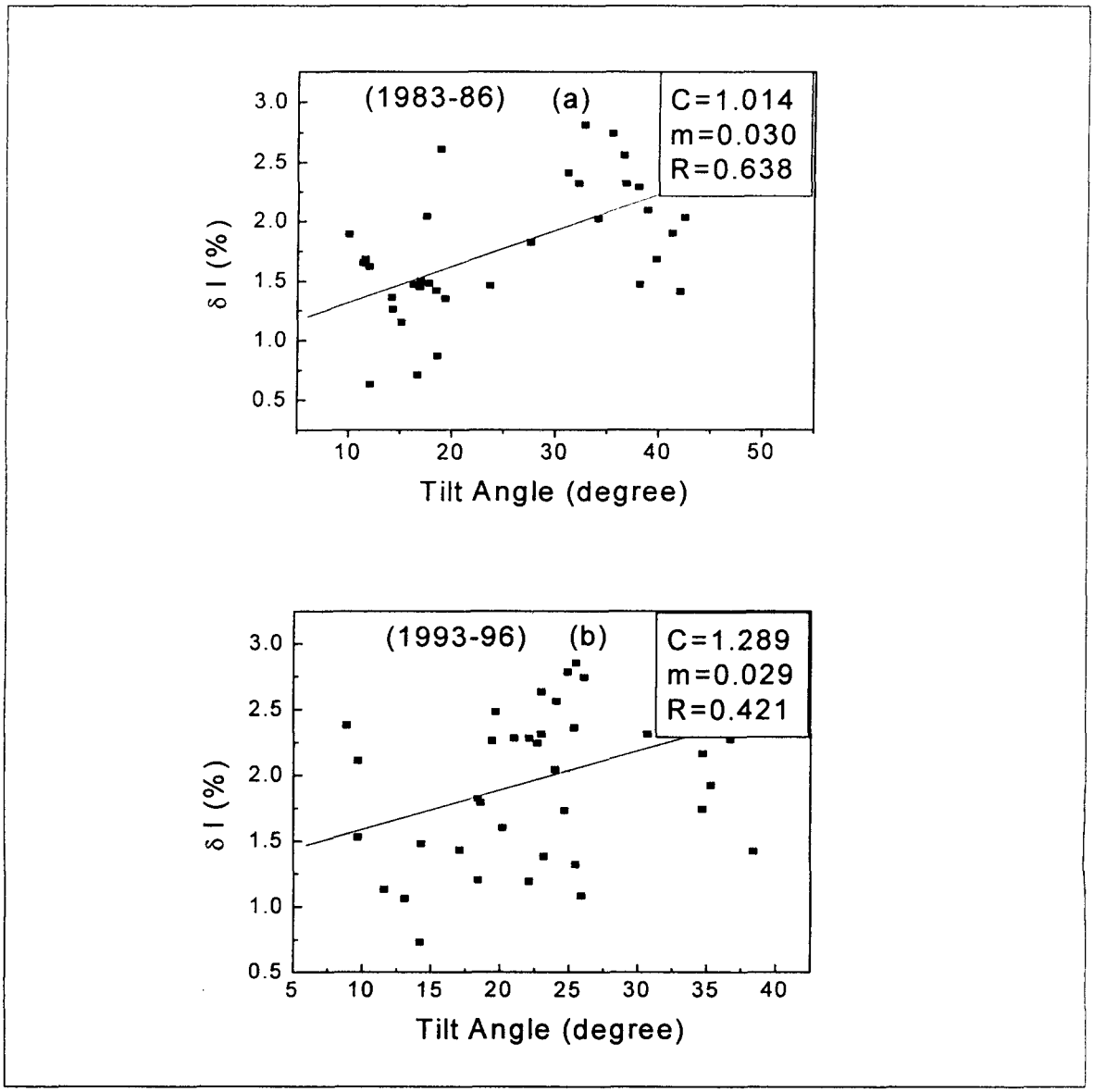

Fig. 2.11: Amplitude of GCR oscillations and relationship with tilt angle of HCS during two different polarity states of the heliosphere in low solar activity periods, (a) 1983-86 and (b) 1993-96.

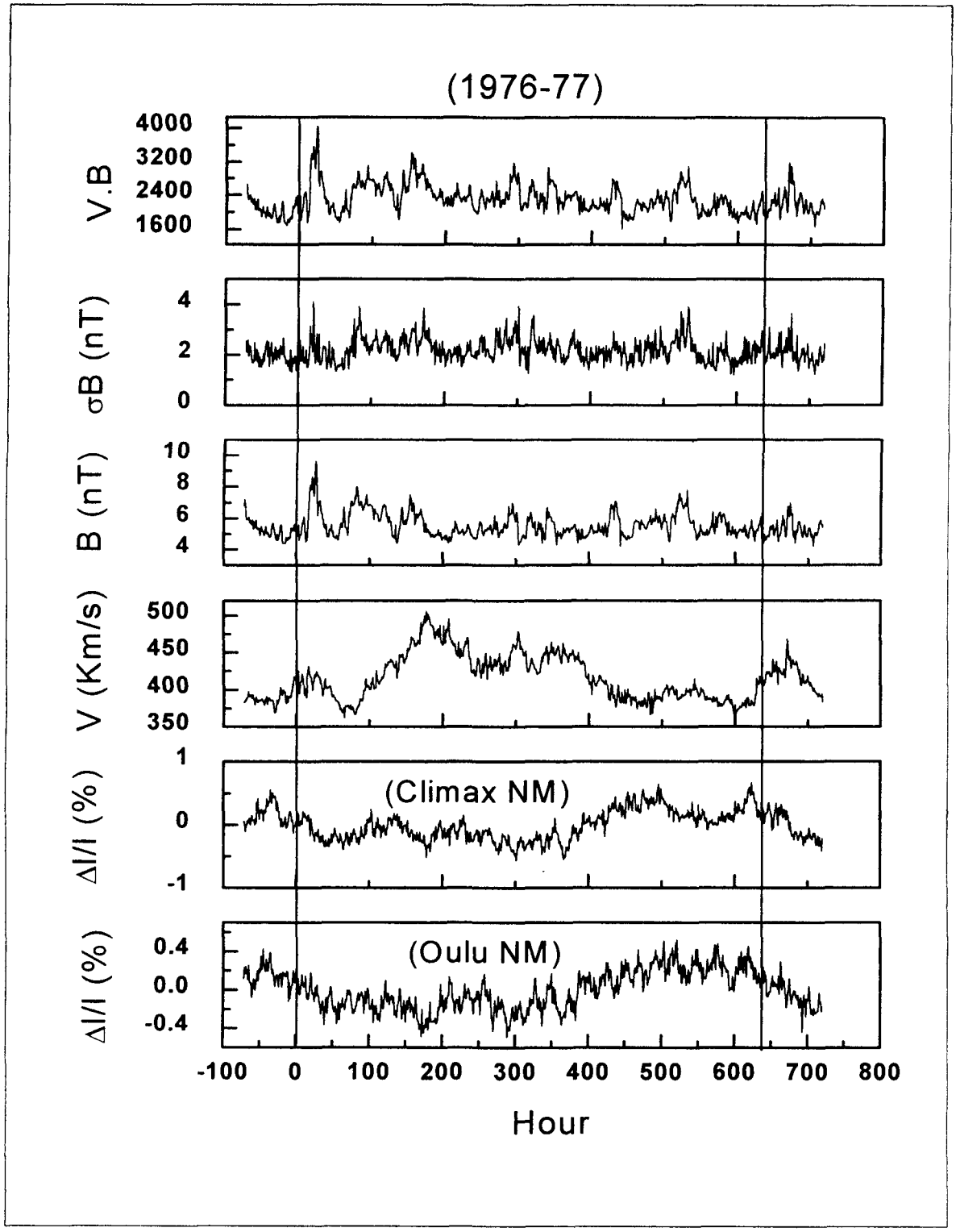

Fig. 2.12(a): Superposed epoch analysis results of hourly cosmic ray data and solar wind plasma/field data showing variations during Carrington rotation periods of minimum solar activity 1976-77 when heliosphere was in A > 0 polarity state; zero hour corresponds to beginning of each Carrington rotation.

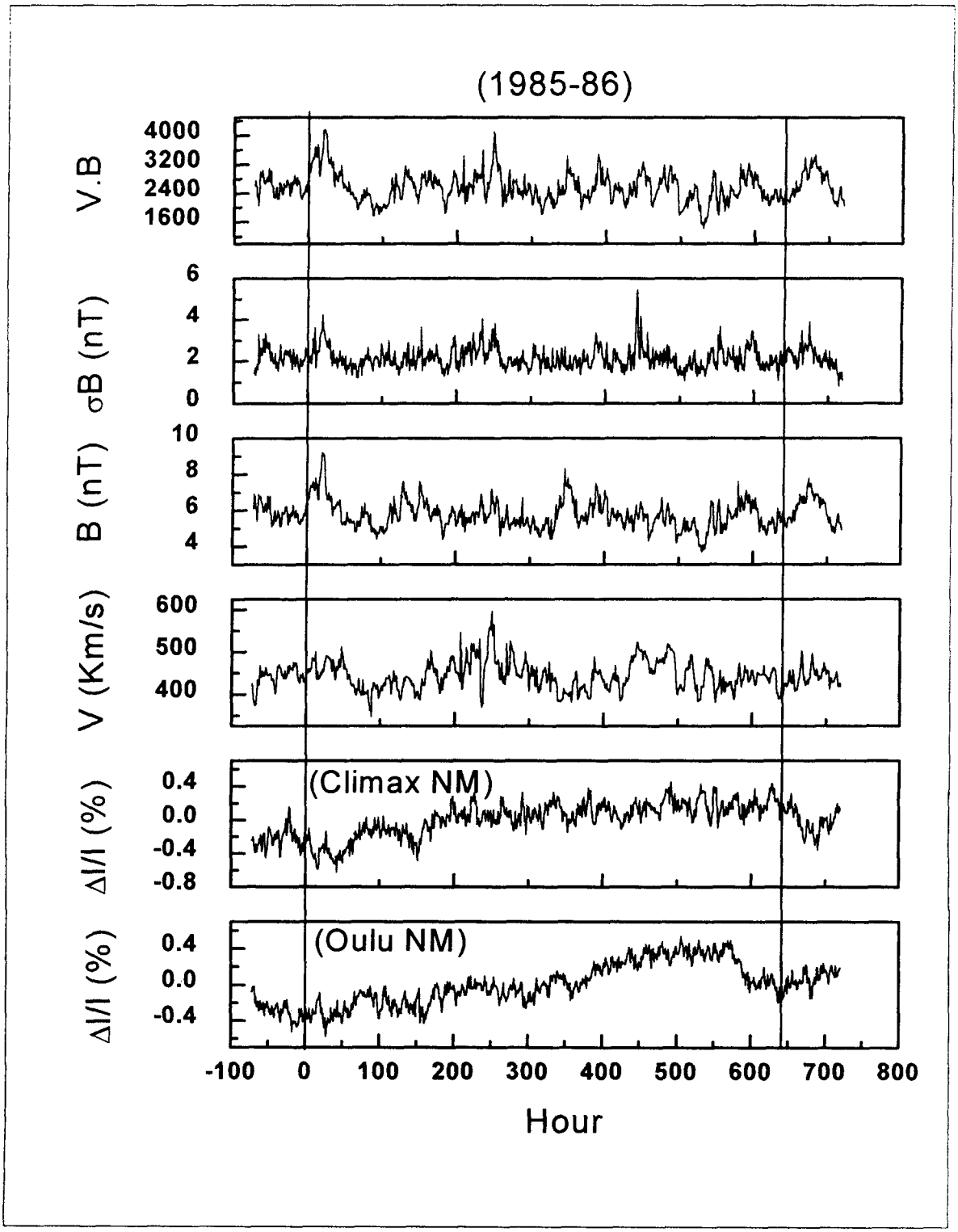

Fig. 2.12(b): Superposed epoch analysis results of hourly cosmic ray data and solar wind plasma/field data showing variations during Carrington rotation periods of minimum solar activity 1985-86 when heliosphere was in A < 0 polarity state; zero hour corresponds to beginning of each Carrington rotation.

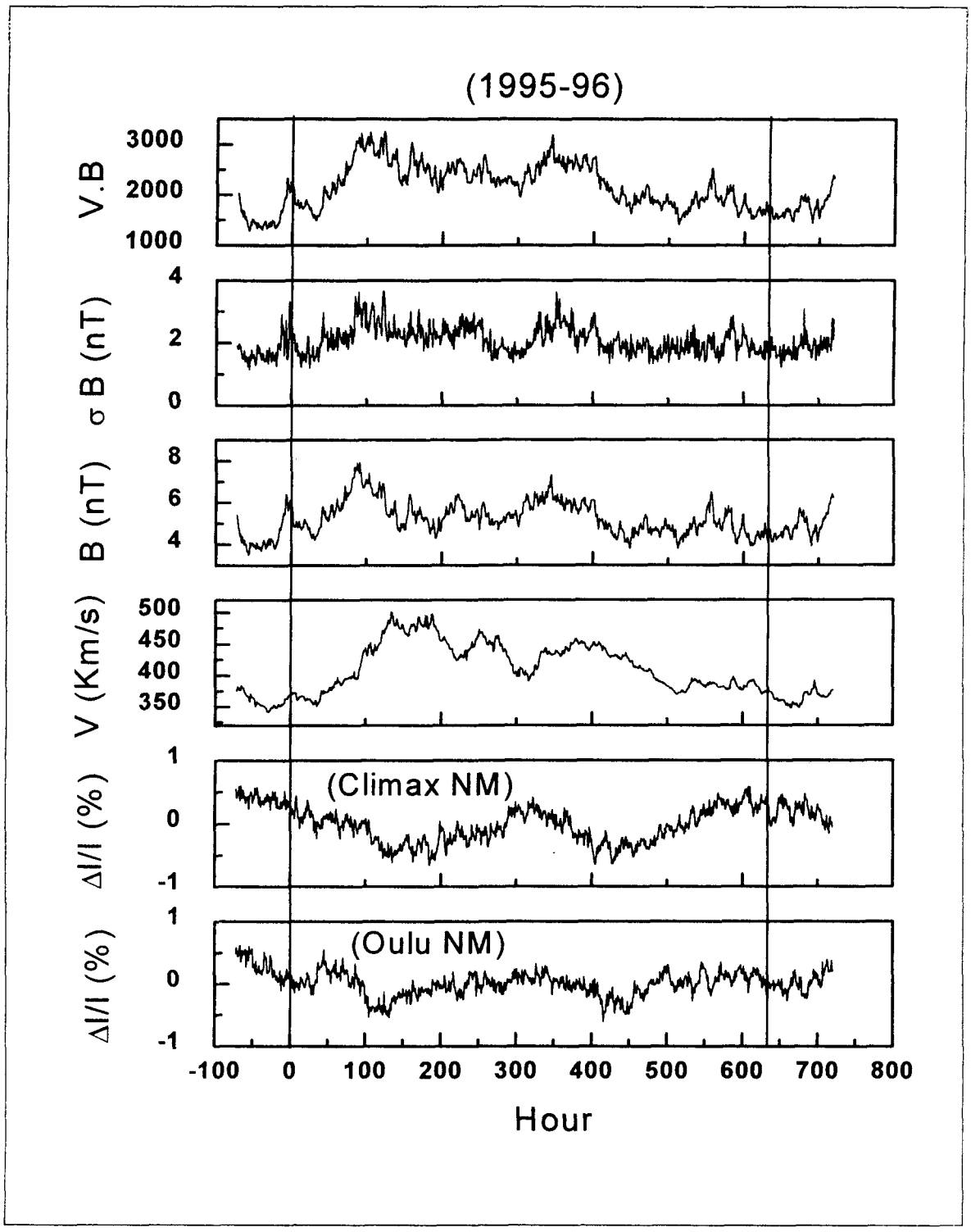

Fig. 2.12(c): Superposed epoch analysis results of hourly cosmic ray data and solar wind plasma/field data showing variations during Carrington rotation periods of minimum solar activity 1995-96 when heliosphere was in A > 0 polarity state; zero hour corresponds to beginning of each Carrington rotation.

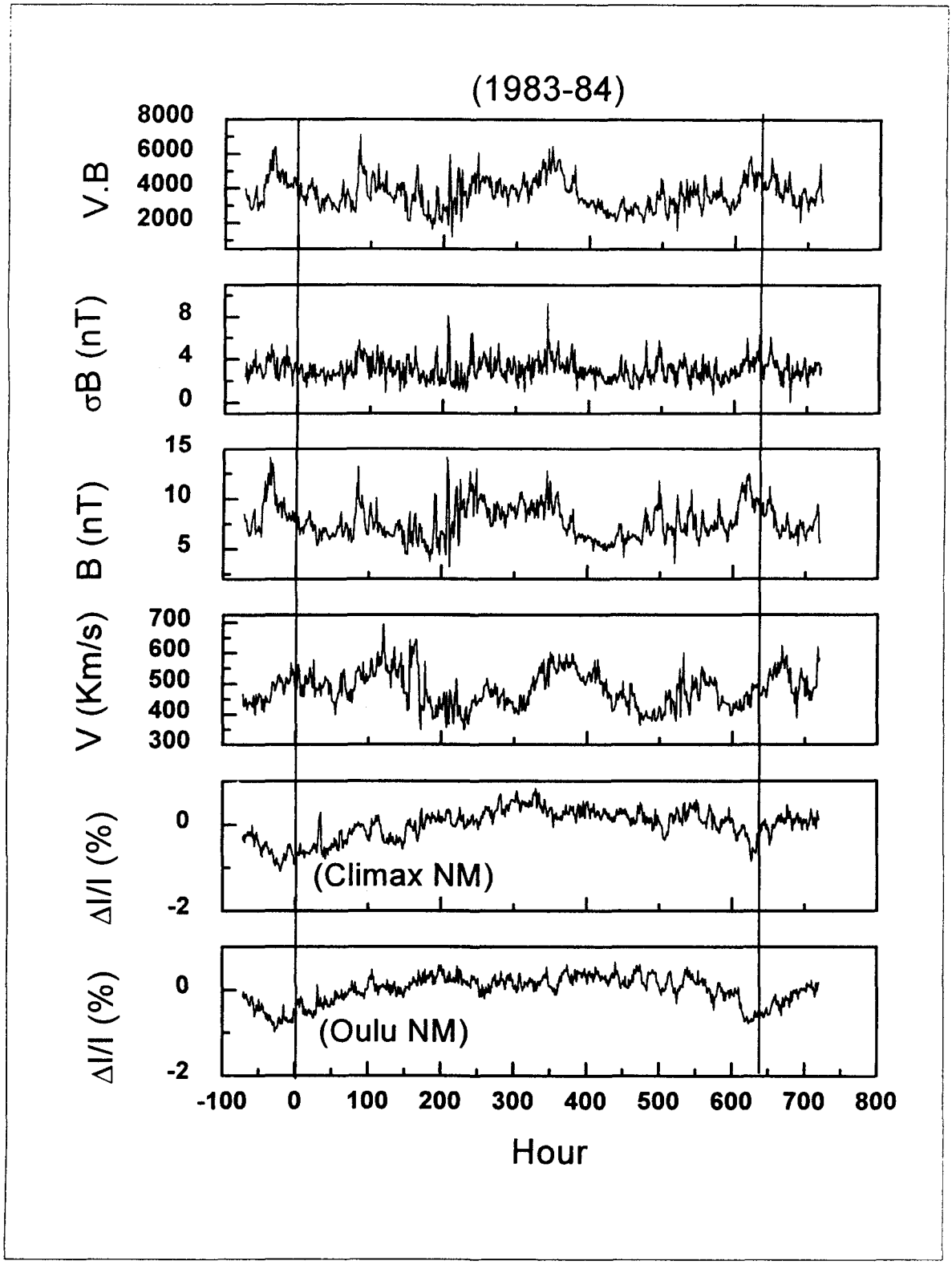

Fig. 2.13(a): Hour-to-hour variations of cosmic ray and solar wind plasma/field data during Carrington rotation in a period of decreasing and low solar activity conditions (1983-84) when A < 0.

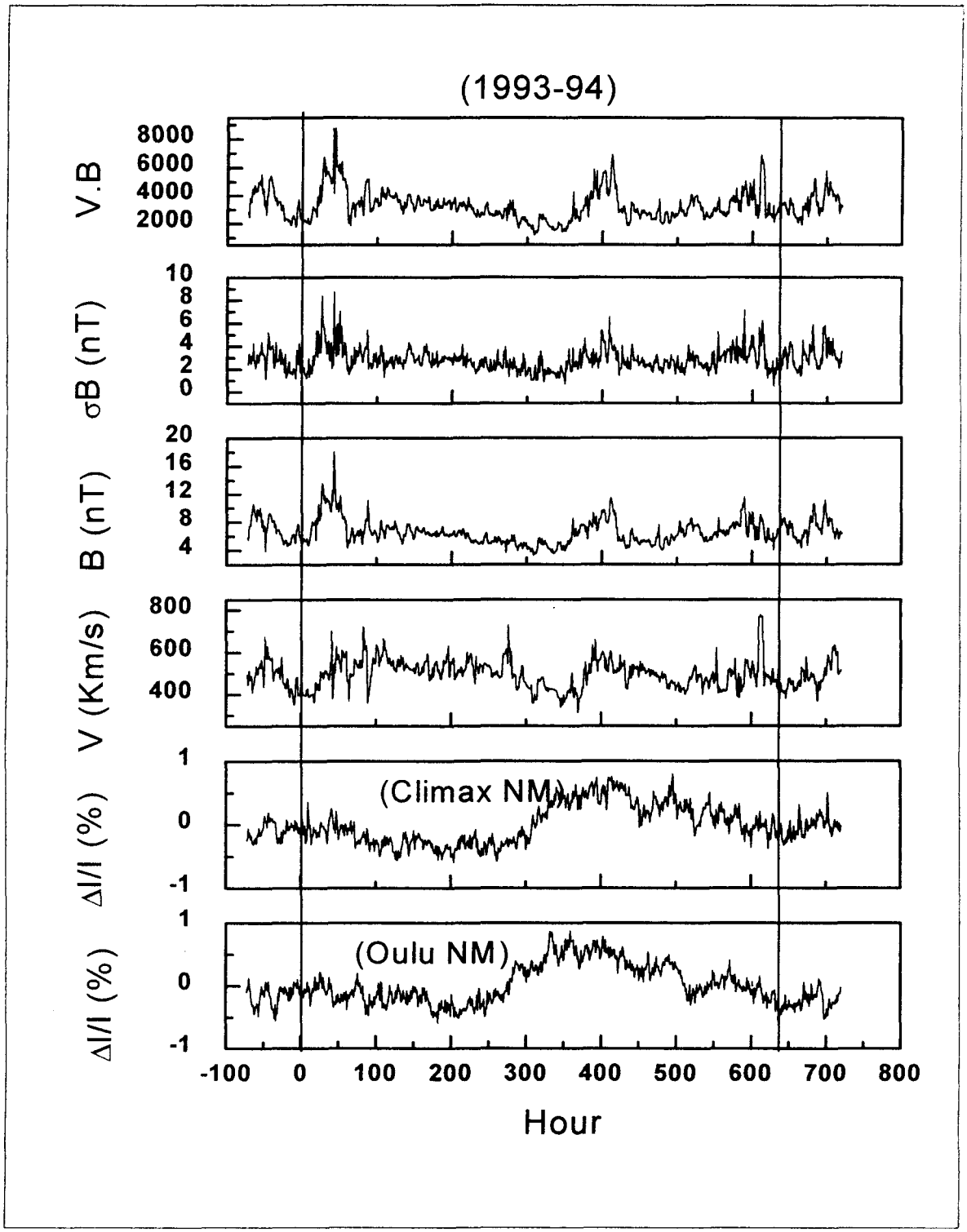

Fig. 2.13(b): Hour-to-hour variations of cosmic ray and solar wind plasma/field data during Carrington rotation in a period of decreasing and low solar activity conditions (1993-94) when A > 0.

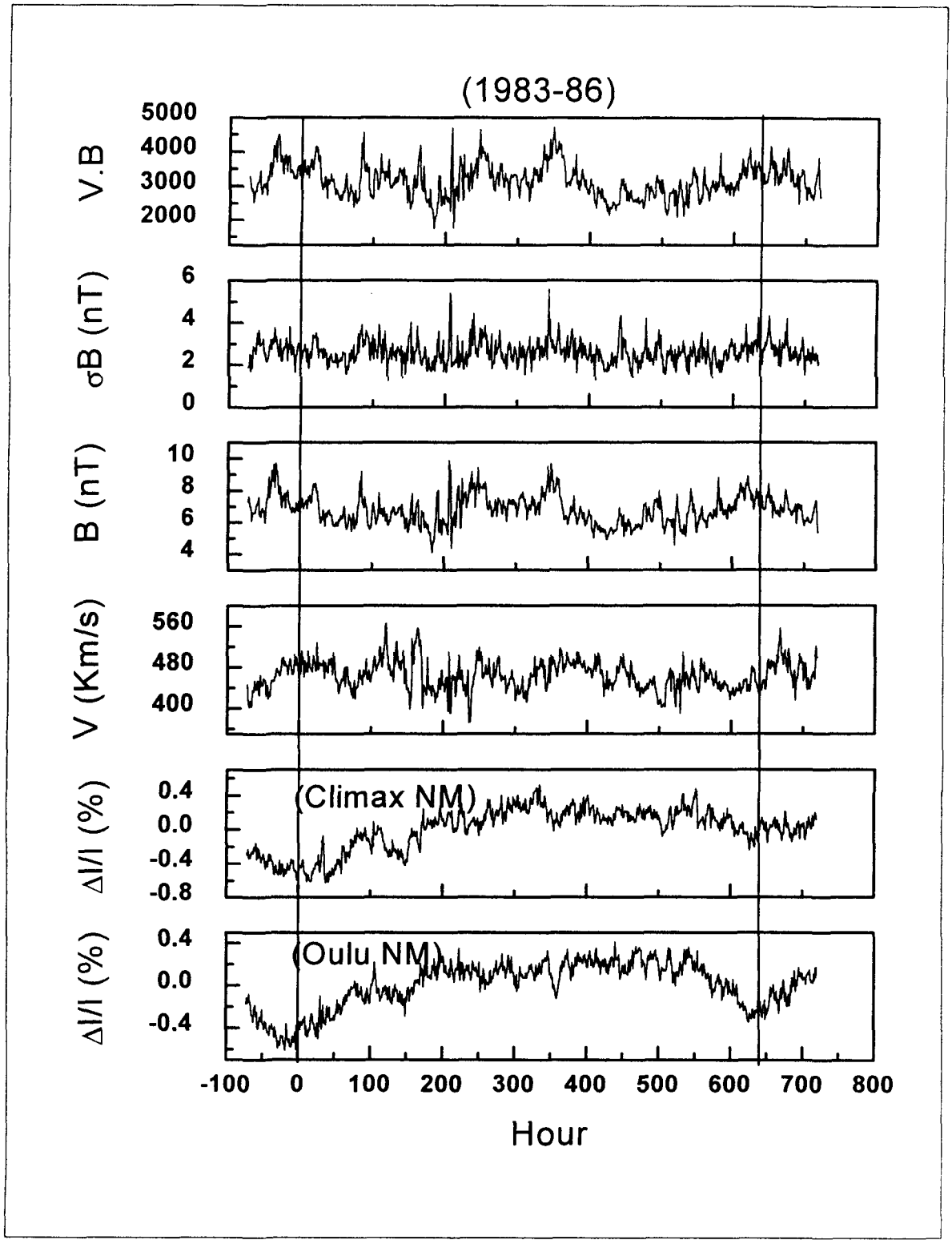

Fig. 2.14(a): Hourly cosmic ray and solar wind data, subjected to superposed epoch analysis with respect to time (hour) of start of Carrington rotation, showing their variations in a period of low solar activity (1983-86) when heliosphere is in A < 0 state.

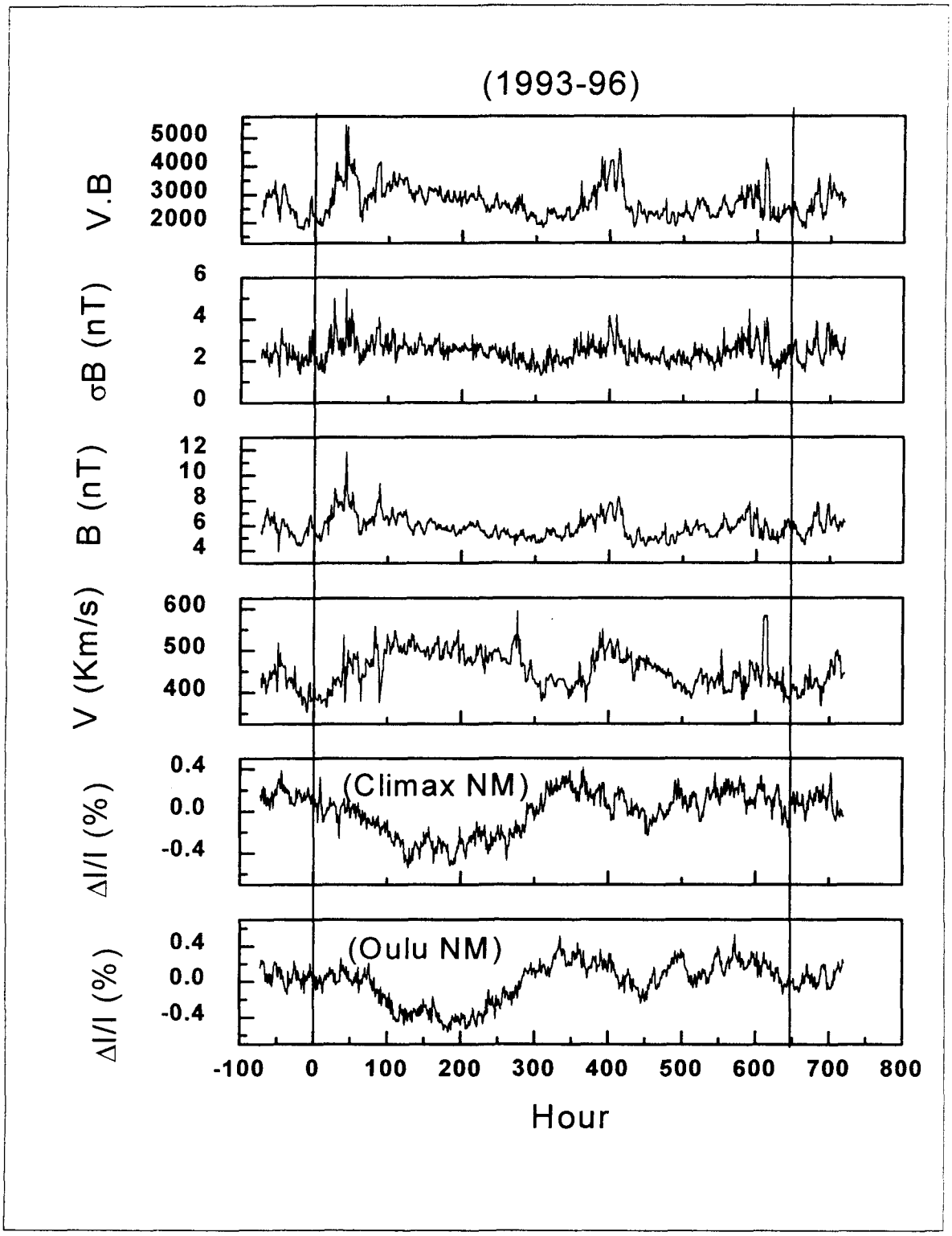

Fig. 2.14(b): Hourly cosmic ray and solar wind data, subjected to superposed epoch analysis with respect to time (hour) of start of Carrington rotation, showing their variations in a period of low solar activity (1993-96) when heliosphere is in A > 0 state.

It is observed from Figs 2.12(a, b, c), 2.13(a, b) and 2.14(a, b) that, in general, time profile of various parameters is in agreement with corresponding parameters of the same periods obtained by analyzing daily average data, shown in Fig. 2.1(a, b, c), 2.5(a, b) and 2.9(a, b). In addition to this general agreement, we also see some additional features/short-term fluctuations in GCR intensity and simultaneous variations in some solar parameters e.g. solar wind velocity, IMF strength and its variance. These superimposed fluctuations over the corotating variations are representative of transient fluctuations in solar wind plasma/field parameters.

Analysis based on daily average data has shown that solar wind velocity is better correlated with GCR intensity during the course of Carrington rotations, at least during A > 0 epochs, (this behaviour can be qualitatively seen in Figs 2.12-2.14 also), however, we did the regression analysis between GCR intensity and solar wind parameters during different periods, using hourly average data also. These values are given in Table-7, 8 and 9.

Table-7: Correlation coefficients between GCR intensity and solar wind plasma/field parameters obtained from hourly data during three solar minimum periods, two in A > 0 epochs and one in A < 0 epoch

Periods	I Vs V	I Vs B	I Vs σB	I Vs (V.B)
1976-77	-0.58	-0.02	-0.13	-0.29
1985-86	-0.007	-0.23	-0.04	-0.20
1995-96	-0.50	-0.15	-0.22	-0.34

Table-8: Correlation coefficients between GCR intensity and solar wind plasma/field parameters obtained from hourly data during two solar minimum periods, one lying in A > 0 epochs and one in A < 0 epoch

Periods	I Vs V	I Vs B	I Vs σB	I Vs (V.B)
1983-84	-0.09	-0.30	-0.16	-0.33
1993-94	-0.20	-0.17	-0.11	-0.19

Table-9: Correlation coefficients between GCR intensity and solar wind plasma/field parameters obtained from hourly data during two solar minimum periods, one lying in A > 0 epochs and one in A < 0 epoch

Periods	I Vs V	I Vs B	I Vs σB	I Vs (V.B)
1983-86	-0.12	-0.30	-0.13	-0.33
1993-96	-0.47	-0.006	-0.09	-0.18

Again, we see that better correlation exists between solar wind velocity and GCR intensity during A > 0 epochs. The regression plots of the GCR intensity variation with solar wind velocity are shown in Fig. 2.15 for 1976-77, 1985-86 and 1995-96 solar minimum period; in Fig. 16 for the periods preceding minimum activity i.e. 1983-84 and 1993-94; in Fig. 2.17 for combined low activity periods i.e. 1983-86, and 1993-96.

Higher time resolution plots shown in Fig. 2.15, 2.16 and 2.17 give additional support and better representation to the conclusions drawn on the basis of Figs. 2.2, 2.6, and 2.11; an important conclusion being an anti-correlation between GCR intensity and solar wind velocity only in A > 0 epochs.

Various models have been developed to account for the observed corotating decreases and their various features. However, so far as the physical processes mainly responsible for this phenomenon are concerned, emphasis differs from one model to the other. Barouch and Burlaga (1975) suggested that enhanced drifts of particles out of the region of enhanced magnetic field associated with corotating interaction region might cause the cosmic rays depression associated with high-speed streams. Scholar et al. (1979) in their model put emphasis on charges in solar wind parameter and magnetic field turbulence in the CIR to explain corotating decreases. Badruddin et al. (1985), Newkirk and Fisk (1985) proposed that recurrent modulation of cosmic rays near ecliptic arise because of latitudinal cosmic ray density gradient that are arranged about tilted heliospheric current sheet. Kota and Jokipii (1991) in their 3-D modulation model including CIR assumed that particle scattering increases with the magnetic field in the vicinity of CIR. To account for the 22-year variation in corotating decreases, Kota and Jokipii (2001) considered a southward-displaced heliospheric current sheet. Richardson et al. (1996) modeled corotating decreases in steady state convection diffusion model and suggested enhanced convection of cosmic rays by high-speed streams (see also Badruddin and Yadav, 1985). On the basis of solution to

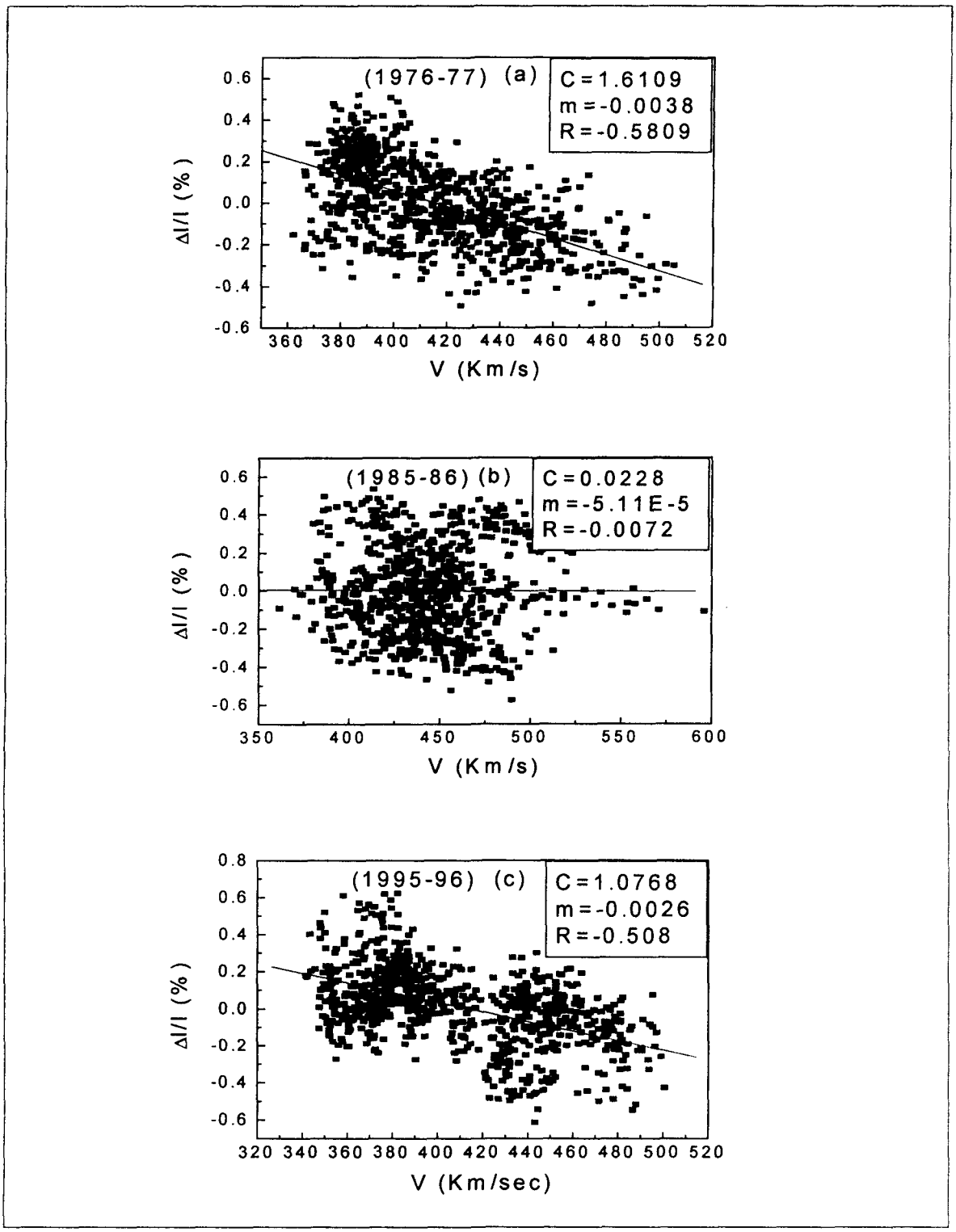

Fig. 2.15 Relationship between change in GCR intensity and solar wind velocity during the course of Carrington rotations in solar minimum periods 1976-77, 1985-86 and 1995-96.

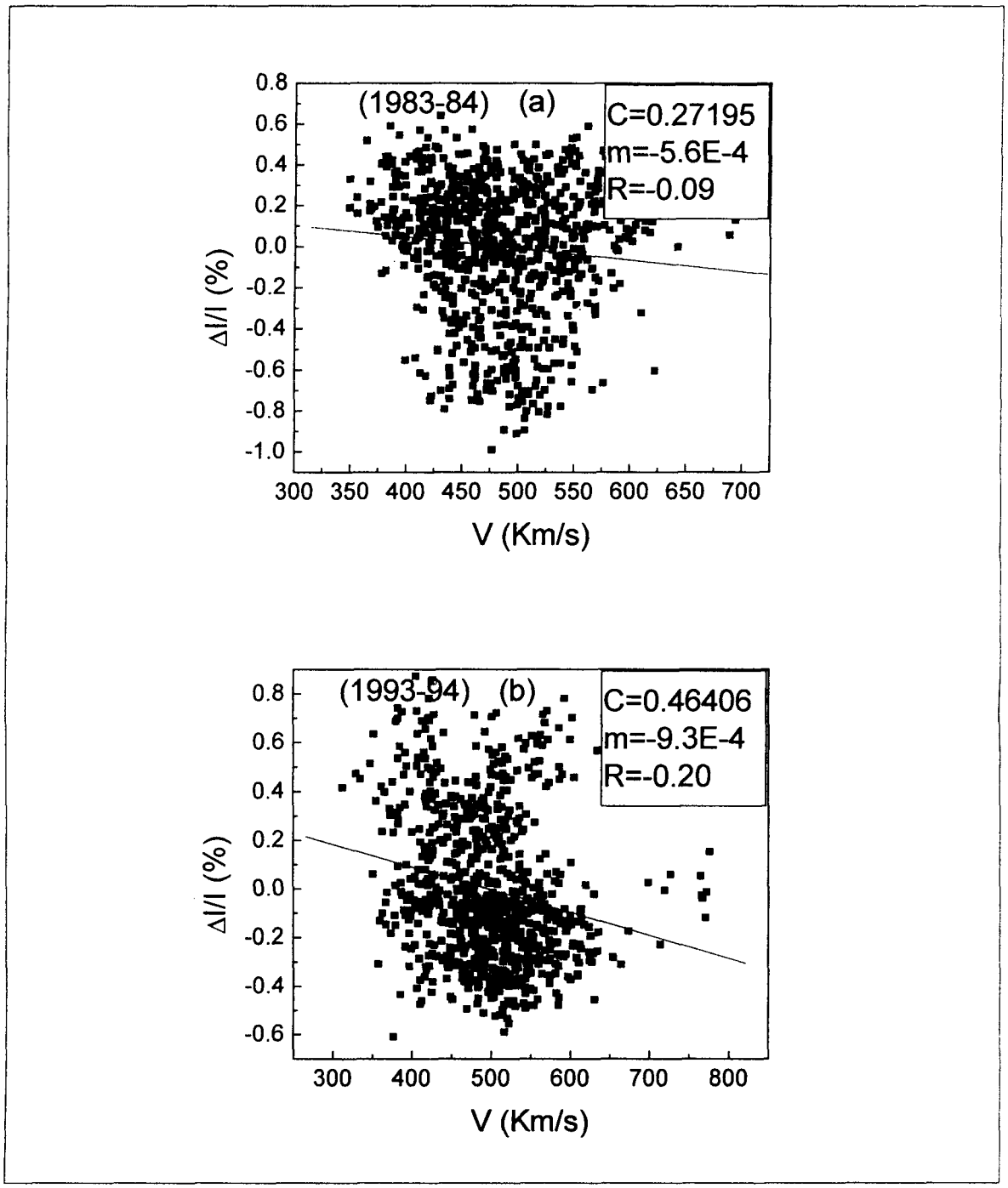

Fig. 2.16 Relationship between change in GCR intensity and solar wind velocity during the course of Carrington rotations in solar minimum periods 1983-84 and 1993-94.

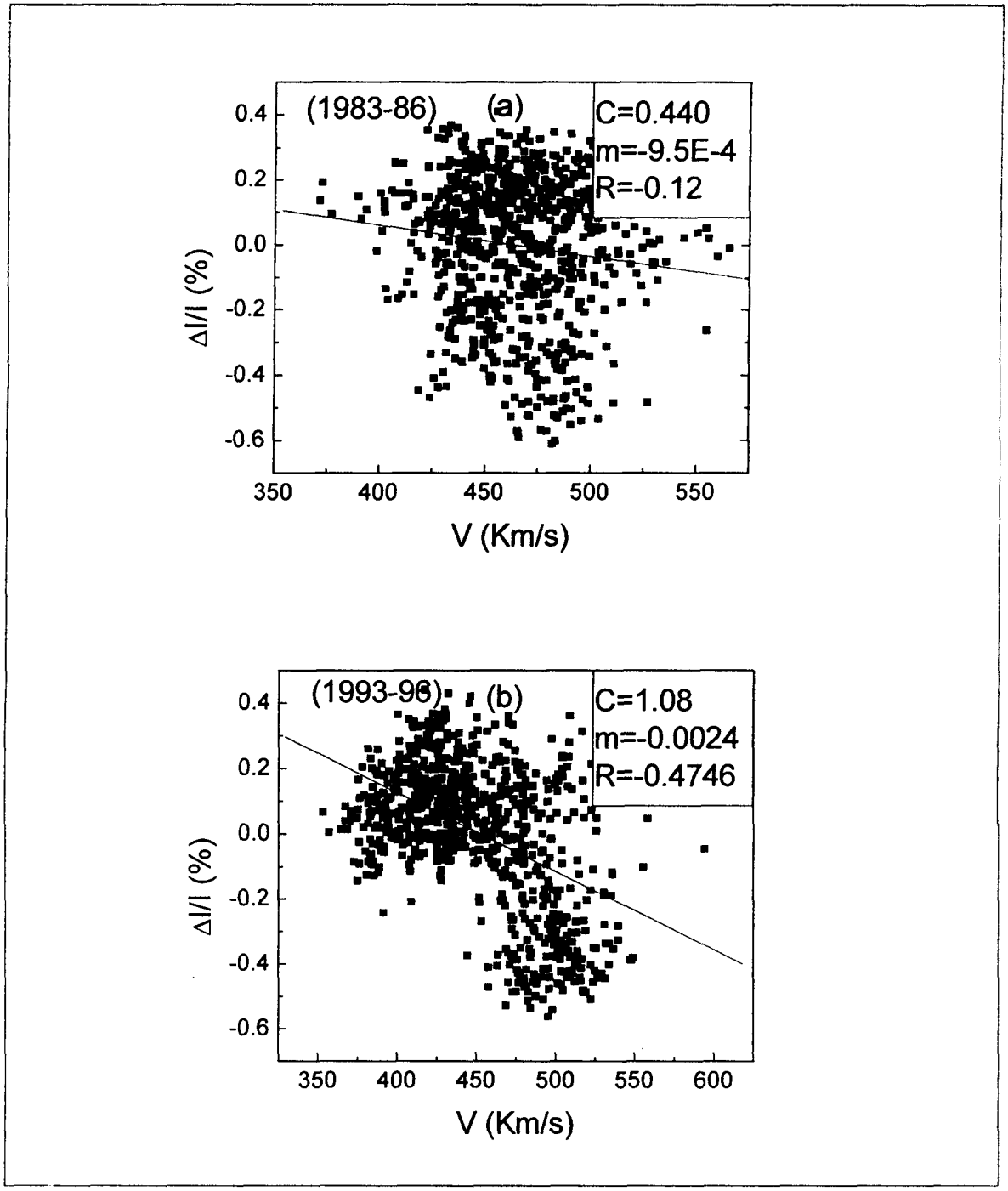

Fig. 2.17 Relationship between change in GCR intensity and solar wind velocity during the course of Carrington rotations in solar minimum periods 1983-86 and 1993-96.

a 3-D transport equation including drifts, Gil and Alania (2001) predicted that the phase of the 22-year variation with respect to HCS may reverse at larger distances in the heliosphere so that larger variations are seen when A < O. More recently, Burger and Hitge (2004) developed a divergence-free Fisk-Parker hybrid heliospheric field using a steady state 3-D modulation model, and investigated the 26-day recurrent variation. They have shown that hybrid field reduces intensities compared to Parker field when qA > 0, with q the sign of the particle charge, and that the reduction is more at low energies than at higher energies. When A < 0, the global effect of hybrid field are almost negligible.

2.4 Conclusions

Study of galactic cosmic ray (GCR) during Carrington rotation periods in low solar activity conditions and in different polarity conditions (A < 0) and (A > 0) leads to the following conclusions:

1. GCR intensity oscillates during the course of Carrington rotation.
2. The solar wind velocity, interplanetary magnetic field strength and its variance vary during the course of Carrington rotation.
3. The average amplitude of GCR-oscillations during Carrington rotations is larger in A > 0 epoch than A < 0 epoch, as observed during solar minimum periods.
4. GCR intensity and solar wind speed tend to show a good (anti) correlation during A > 0 but are poorly correlated during A < 0.
5. The amplitudes of GCR-oscillations during Carrington rotations show some dependence on the tilt angle of the heliospheric current sheet. However, this dependence is similar for both the polarity epochs, A < 0 and A > 0 with nearly same density gradient in GCR with tilt angle in both the polarity epochs.

References

References

Alania, M.V., Baranov, D.G., Tyasto, M.L. and Vernova, E.S., *Adv. Space Res.*, **27**, 619(2001).

Badruddin, Yadav, R.S. and Yadav, N.R, *Planet. Space. Sci.*, **33**, 191(1985).

Badruddin, *Astrophys. Space Sci.*, **246**, 171(1997).

Badruddin, *Proc. 23rd Int. Cosmic Ray Conf.*, **3**, 727(1993).

Barnes, A., *Rev. Geophys.*, **30**, 43(1992).

Barounch, E. and Burlaga, L.F., *J. Geophys. Res.*, **80**, 449(1975).

Burger, R.A. and Hitge, M., *Astrophys. J.*, **617**, L76(2004).

Burlaga, L.F., McKibben, F.B., Ness, N.F., Schwenn, R., Lazarus, A.J. and Mariani, F., *J. Geophys. Res.*, **89**, 6579(1984).

Burlaga, L.F., et al., *J. Geophys. Res.*, **98**, 17451(1993).

Chen, J. and Bieber, J.W., *Astrophys. J.*, **405**, 375(1993).

Cummings, A.C. and Stone, E.C., *Proc. 6th Int. Solar Wind Conf.*, **2**, 599(1988).

Duggal, S.P. and Pomerantz, M.A., *Proc. 15th Int. Cosmic Ray Conf.*, **3**, 370(1977).

Duggal, S.P., Tsurutani, B.T., Pomerantz, M.A., Tsao, C.H. and Smith, E.J., *J. Geophys. Res.*, **86**, 7473(1981).

Earl, J.A., Jokipii, J.R. and Morfill, G.M., *Astrophys. J.*, **331**, L91(1988).

Fisk, L.A., *J. Geophys. Res.*, **101**, 15547(1996).

Forbush, S.E., *Phys. Rev.*, **54**, 975(1938).

Gil, A., Iskra, *K.*, Modzelewska, R. and Alania, M.V., *Adv. Space Res.*, (in Press)(2005).

Gil, A. and Alania, M.V., *Proc 21st Int. Cosmic Ray Conf.*, **9**, 3725(2001).

Gosling, J.T., *Annu. Rev. Astron. Astrophys.*, **34**, 35(1996).

Gupta, V. and Badruddin, *Proc. 29th Int. Cosmic Ray Conf.*, SH 3.2 (in press)(2005).

Heber, B. and Burger, R.A., *Space Sci. Rev.*, **89**, 125(1999).

Iucci, N., Parisi, M., Storini, M. and Villoresi, G., *Nuovo Cim.*, **2**, 421(1979).

Jokipii, J.R., *Adv. Space Res.*, **9**, 105(1989).

Jokipii, J.R. and Kota, J., *Geophys. Res. Lett.*, **16**, 1(1989).

Jokipii, J.R., Levy, E.H. and Hubbard, W.B., *Astrophys. J.*, **213**, 861(1977).

Kallenrode, May-Britt, *Space Physics,* Springer-Verlag (1998).

Kota, J. and Jokipii, J.R, *Astrophys. J.*, **265**, 573(1983).

Kota, J., *Proc. 1st COSPAR Colloquium*, Grzedzielski, S., and Page, D.E., (eds), Pergamon Press, p. 119(1989).

Kota, J. and Jokipii, J.R, *Geophys. Res. Lett.*, **18**, 1797(1991).

Kota, J. and Jokipii, J.R, *Proc. 21st Int. Cosmic Ray Conf.*, **9**, 3577(2001).

Kurth, W.S. and Gurnett, D.A., *Geophys. Res. Lett.*, **18,** 1801(1991).

McDonald, F.B., Lal, N. and McGuire, R.E., *J. Geophys. Res.*, **98**, 1243(1993).

Mckibben, R.B., et al., *Space Sci. Rev.*, **89**, 307(1999).

Mckibben, R.B., et al., Cosmic Ray Modulation, in *Proc.6th Int. Solar Wind Conf.*, Pizzo, V.J., Holzer, T.E. and Sime, D.E., (eds)(1988).

Mckibben, R.B., et al., *Space Sci. Rev.*, **72**, 367(1995).

Mckibben, R.B., et al., *Proc. 1st COSPAR Colloquium*, Grzedzielski, S., and Page, D.E., (eds), Pergamon Press, p. 107(1990).

Meyer, P., Parker, E.N. and Simpson, J.A., *Phys. Rev.*, **104**, 768(1956).

Mishra, B.L., Shrivastava, P.K. and Agrawal, S.P., *Proc. 21st Int. Cosmic Ray Conf.*, **6**, 299(1990).

Newkirk, G. and Fisk. L.A., *Geophys. Res. Lett.*, **8**, 619(1981).

Newkirk, G. and Fisk. L.A., *J. Geophys. Res.*, **90**, 3391(1985).

Paizis, C., Heber, B., Farrando, P., Raviart, A., Faleoni, B., Marzolla, S., Potgieter, M.S., Bothmer, V., Kunow, H., Muller-Mellin, R. and Posner, A., *J. Geophys. Res.*, **104**, 28241(1999).

Parker, E.N., *Astrophys. J.*, **128**, 664(1958).

Parker, E.N., *Planetary Space Sci.*, **12**, 735(1964).

Parker, E.N., *Planetary Space Sci.*, **13**, 9(1965).

Perko, J.S., *J. Geophys. Res.*, **98**, 19027(1993).

Potgieter, M.S., *Space Sci. Rev.*, **83**, 147(1998).

Potgieter, M.S., *Proc. 23rd Int. Cosmic Ray Conf.*, Leahy, D.A., Hicks, R.B. and Venkatesan, D., (eds), World Scientific Press, p. 213(1994).

Reames, D.V. and Ng., C.K., *Astrophys. J.*, **563**, L179(2001).

Richardson, I.G., *Space, Sci. Rev.*, **121**, 267(2004).

Richardson, I.G., Wibbrenz, G. and Cane, H.V., *J. Geophys. Res.*, **101**, 13,483(1996).

Richardson, I.G., Cane, H.V. and Wibbrenz, G., *J. Geophys. Res.*, **104**, 12,549(1999).

Scholar, M., Hovestadt, D., Klecker, B. and Gloecker, G., *Astrophys. J.*, **227**, 323(1979).

Singh, Y.P. and Badruddin, *Proc. 29th Int. Cosmic Ray Conf.,* SH 3.2 (in press)(2005).

Simnett, G.M., et al., *Space Sci. Rev.,* **83**, 215(1998).

Smith, E.J., *J. Geophys. Res.*, **95**, 18,731(1990).

Smith, E.J., The Sun and Interplanetary Magnetic Field, in *The Sun In Time*, Sonett, C.P., Giampapa, M.S. and Mathews, M.S., (eds)Univ. of Arizona. Press(1993).

Stone, E.C., *Proc. 20th Int. Cosmic Ray Conf.*, **7**, 105(1987).

Venkatesan, D., Shukla, A.K. and Agrawal, S.P., *Solar Phys.,* **81**, 375(1982).

Venkatesan, D. and Badruddin, *Space Sci. Rev.*, **52**, 121(1990).

Webber, W.R. and Lockwood, J.A., *J. Geophys. Res.*, **98**, 21095(1993).

Yadav, RS., Sharma N.K. and Badruddin, *Solar Phys.,* **151**, 393(1994).

Zhang, M., *Astrophys. J.*, **484**, 841(1997).

Zhang, M., Simpson, J. A., Mckibben, R. B., Johns, T. S., Smith, E. J. and Phillips, J. L., *Proc. 24th Int. Cosmic Ray Conf.,* **4**, 956(1995).